The Abdus Salam
International Centre for Theoretical Physics

United Nations
Educational, Scientific and
Cultural Organization

IAEA
International Atomic Energy Agency

SMR/1849-11

Conference and School on Predictability of Natural Disasters for our Planet in Danger. A System View; Theory, Models, Data Analysis

25 June - 6 July, 2007

Similarity and Difference in sequences of solar flares, earthquakes, and starquakes

Vladimir G. Kossobokov

International Institute of Earthquake Prediction Theory
& Mathematical Geophysics, Moscow, Russia
& IGPG, Paris, France

Similarity and Difference in sequences of solar flares, earthquakes, and starquakes

V. Kossobokov

International Institute of Earthquake Prediction Theory

and Mathematcal Geophysics, Russian Federation

Institut de Physique du Globe de Paris, France

F. Lepreti, V. Carbone

Plasma Physics and Astrophysics Group

Dipartimento di Fisica, Università della Calabria, Italy

Introduction and motivation

- Impulsive energy release events occur in many natural systems. Some examples are earthquakes, solar and stellar flares, “neutron-star-quakes”, gamma ray bursts, current disruptions in plasma devices
- Some similarities exist in the statistical properties of these phenomena, e.g. power law distributions of released energy and inter-event times

- Is there a common (“universal”) physical mechanism giving rise to these processes?
- This idea has been considered in particular for earthquakes and solar flares (e.g. the Self Organized Criticality paradigm proposed by Bak et al., 1987, 1988)
- The presence of universality in earthquake and solar flare occurrence has been more recently suggested on the basis of the analogies found in the statistical properties of the temporal sequences of the two phenomena (de Arcangelis et al. 2006)

Introduction and motivation

- In this work we reconsider the question of "universality" in earthquakes and solar flares analyzing the statistical properties of the sequences of events available from the SCSN earthquake catalog and in the GOES flare catalog

- An important technical issue in studies of probability distributions is the binning method. In order to reduce the ambiguities related to the choice of binning we decided to work with cumulative distributions

Earthquakes

- Sudden energy release events in the Earth crust.

  - A coherent phenomenology on seismic events, which we evidence from their consequences, is lacking. Apparently, earthquakes occur through frictional sliding along the boundaries of highly stressed hierarchies of blocks of different sizes (from grains of rock about 10^{-3} m to tectonic plates up to 10^{7} m in linear dimension) that form the lithosphere of the Earth (*Keilis-Borok 1990*).
  - $E = 10^{2} \div 10^{18}$ J (i.e., $M = -2 \div 9$)
  - Earthquakes occur prevalently in seismic regions, i.e. in fault zones.

November 14, 2001, Kokoxili Earthquake along the Kunlun fault in Tibet (Xinhua/China News Agency)

Solar flares

- Sudden energy release events in the solar atmosphere
- Emission observed in a wide frequency range of the E.M. spectrum, from radio waves up to X-rays and γ-rays

- Solar flares are due to the conversion of magnetic energy (accumulated in the solar atmosphere as a consequence of turbulent convective motions) into accelerated particles, heating, plasma flows.
- $E = 10^{17} \div 10^{26}$ J
- Flares occur prevalently in magnetic activity regions

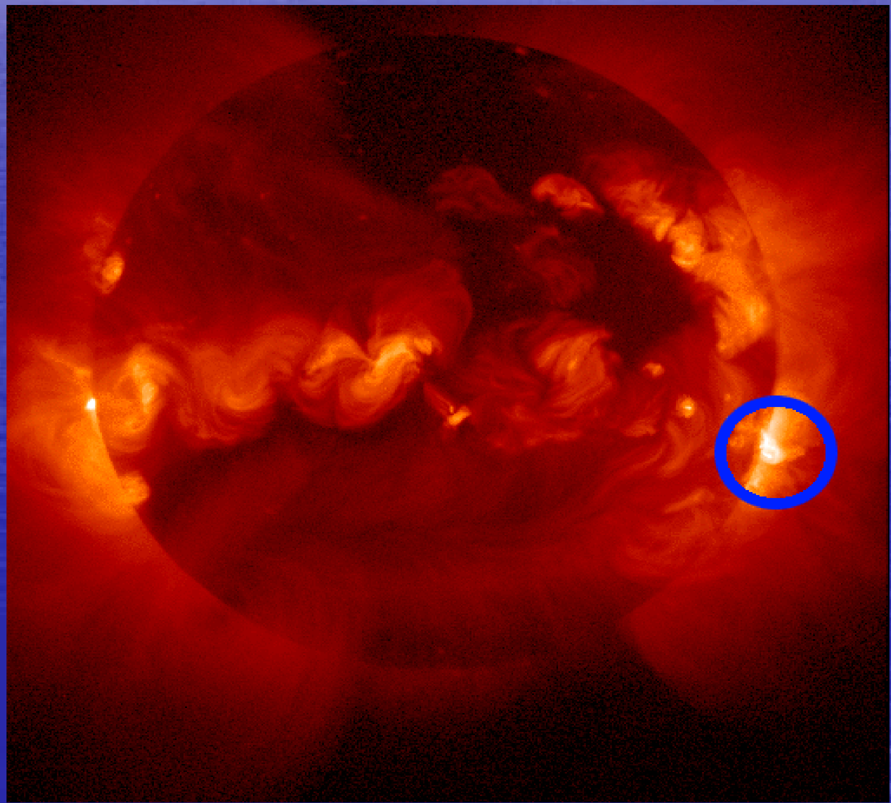

Soft X-ray image of the solar corona (Yohkoh spacecraft)

Data

Earthquake catalog

- Southern California Seismic Network (SCSN) catalog
- Period 1986-2005
- Over 350000 events. About 87000 with $M \geq 2$.

Solar flare catalog

- Compiled from observations of the Geostationary Operational Environmental Satellites (GOES) in the soft X-ray band 1.5-12.4 keV
- Period 1975-2006. Three solar cycles (1975-1986, 1986-1996, 1996-2006).
- Flares classified according to the peak burst intensity I_p in the above band

  B class if $I_p < 10^{-3}$

  C class if $10^{-3} < I_p < 10^{-2}$

  M class if $10^{-2} < I_p < 10^{-1}$

  X class if $I_p > 10^{-1}$

  (Values of I_p given in erg s^{-1} cm^{-2})

  For example a C4.6 class means that $I_p = 4.6 \times 10^{-3}$ erg s^{-1} cm^{-2}
- Over 62000 events. About 32000 of class ≥ C2

Flare peak burst intensity vs. integrated flux

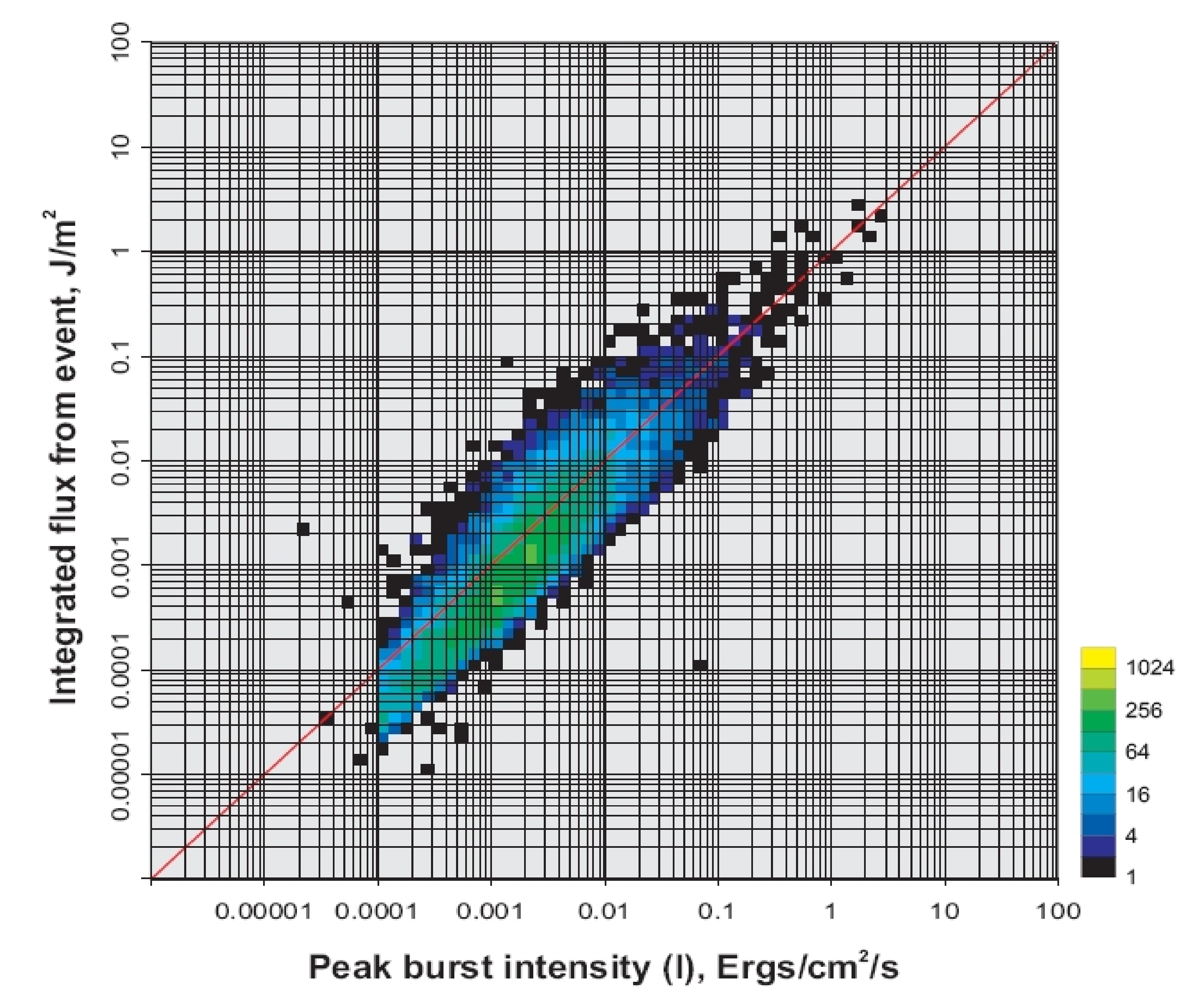

Gutenberg-Richter plots

Solar flares

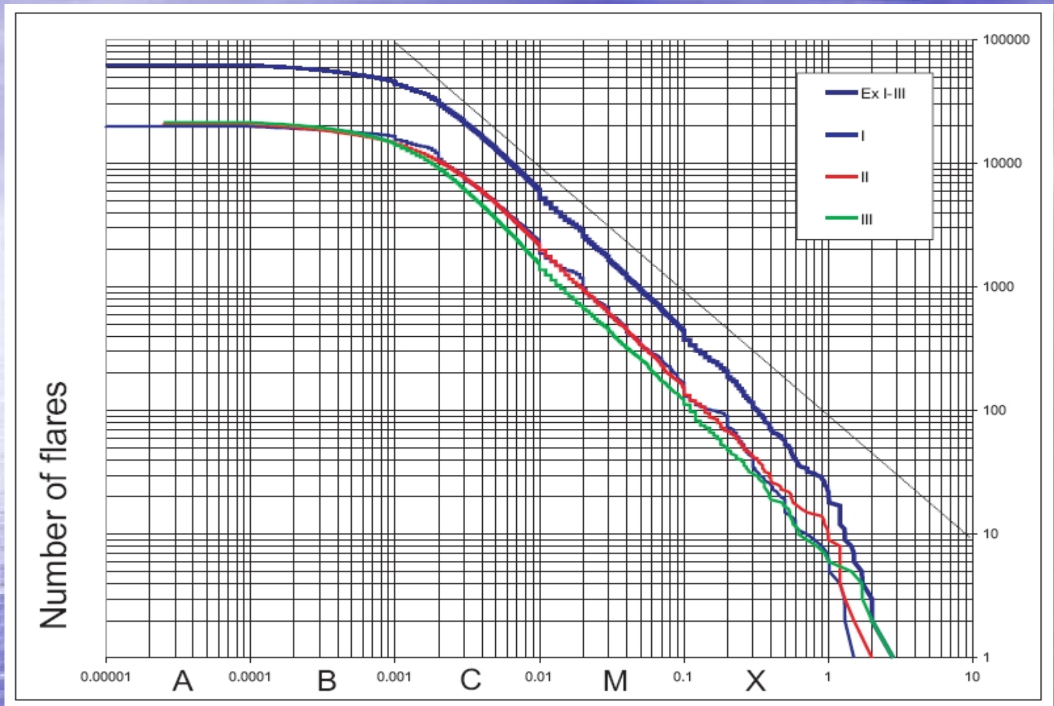

Earthquakes

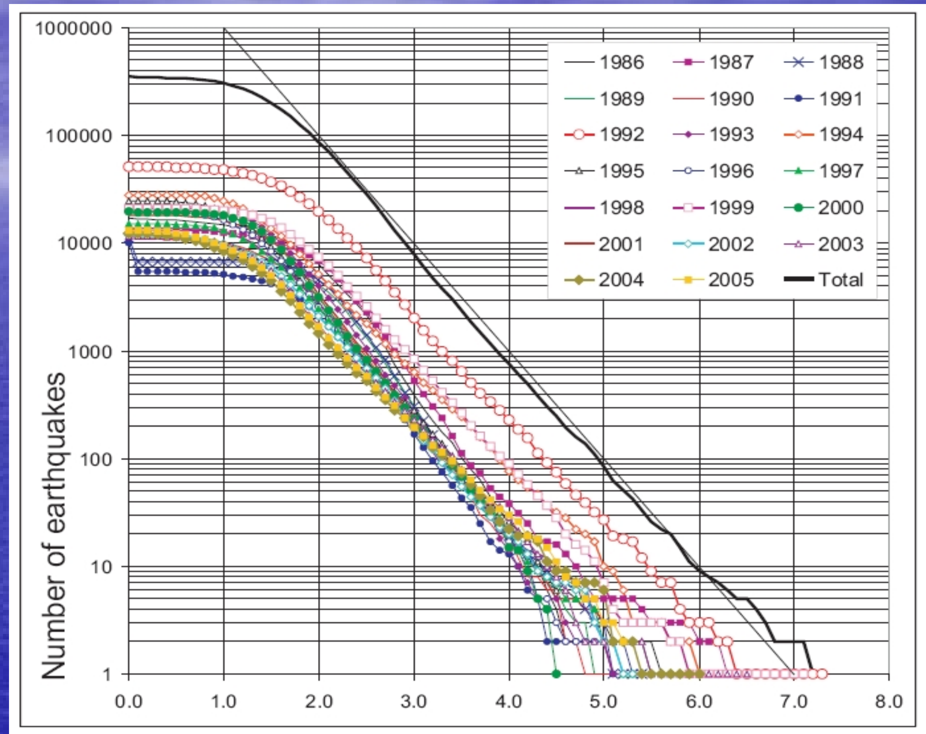

- Lower breakpoints of the power law around C2 class for flares and M2 magnitude for EQs, suggesting incompleteness of the catalogs below these values
- Only events above these thresholds considered in the rest of our analysis

Inter-event times and event magnitude vs. time

Solar flares

Earthquakes

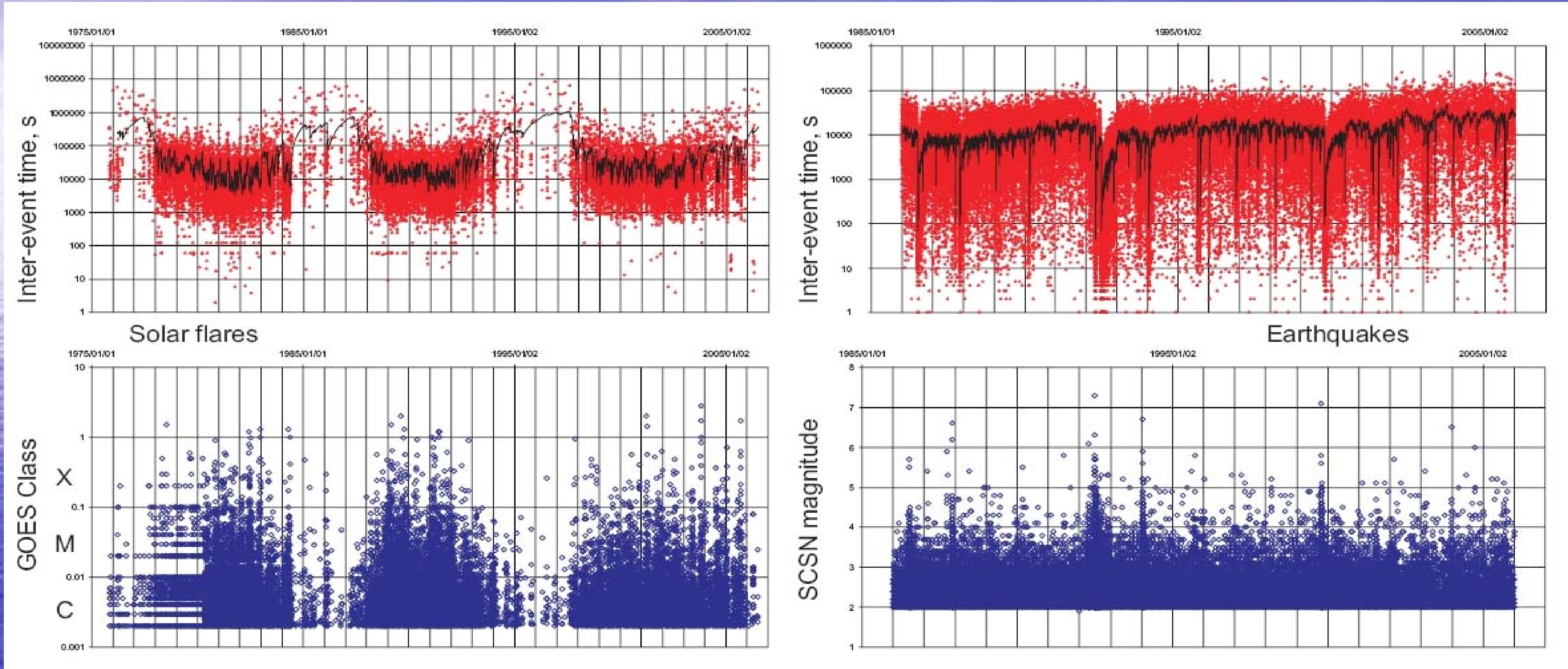

GOES class vs. time

Magnitude vs. time

Magnitude frequencies vs. time

Solar flares

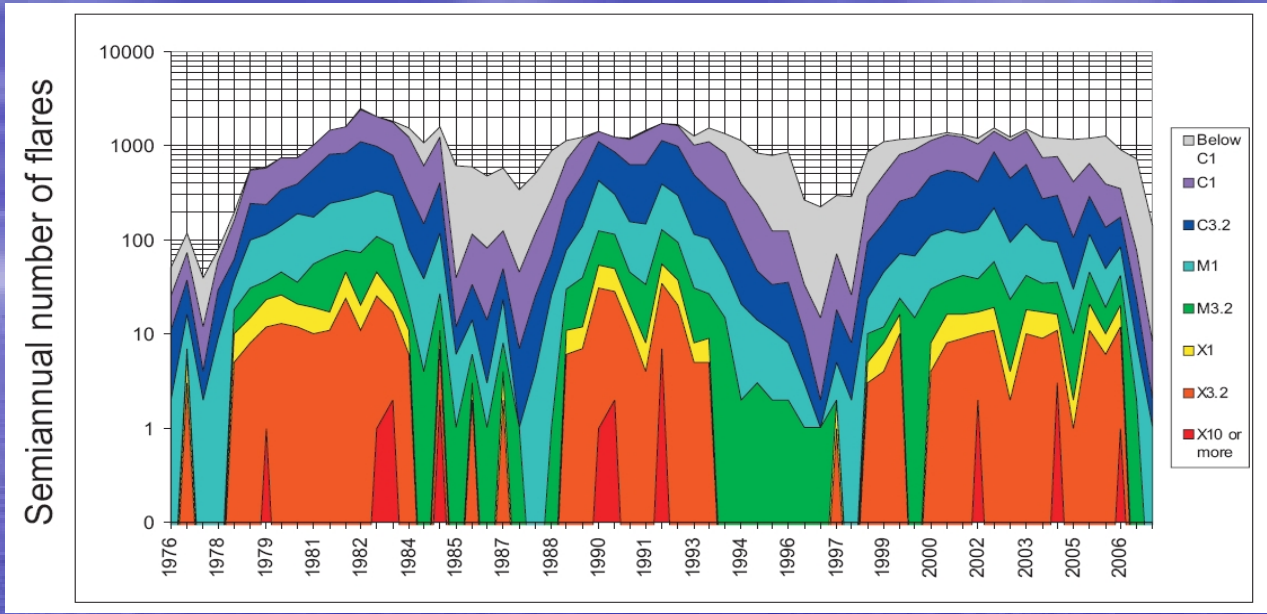

Earthquakes

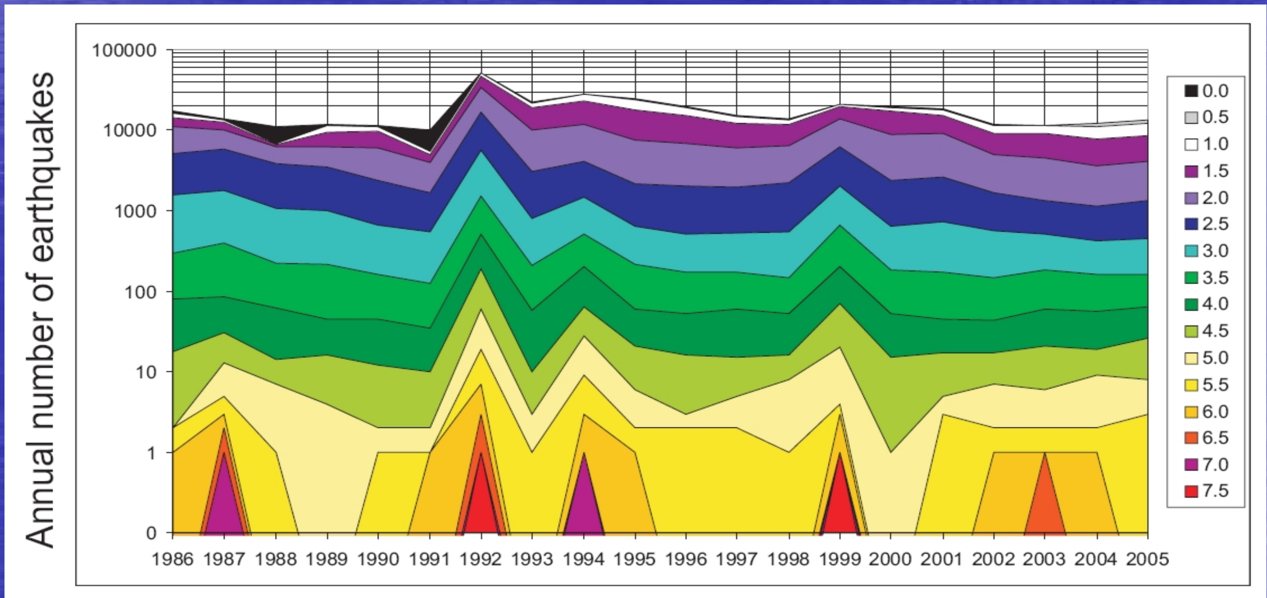

Accumulated number and energy vs. time

Solar flares | Earthquakes

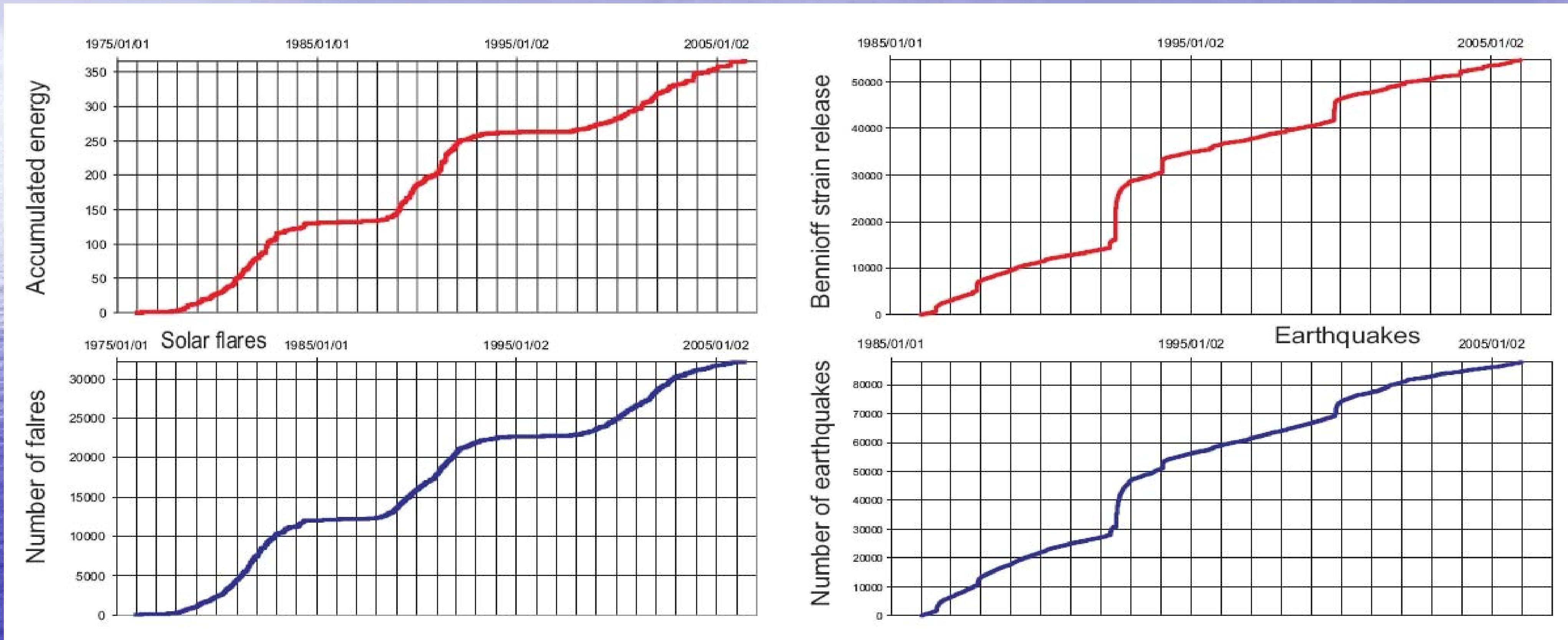

Inter-event time distributions

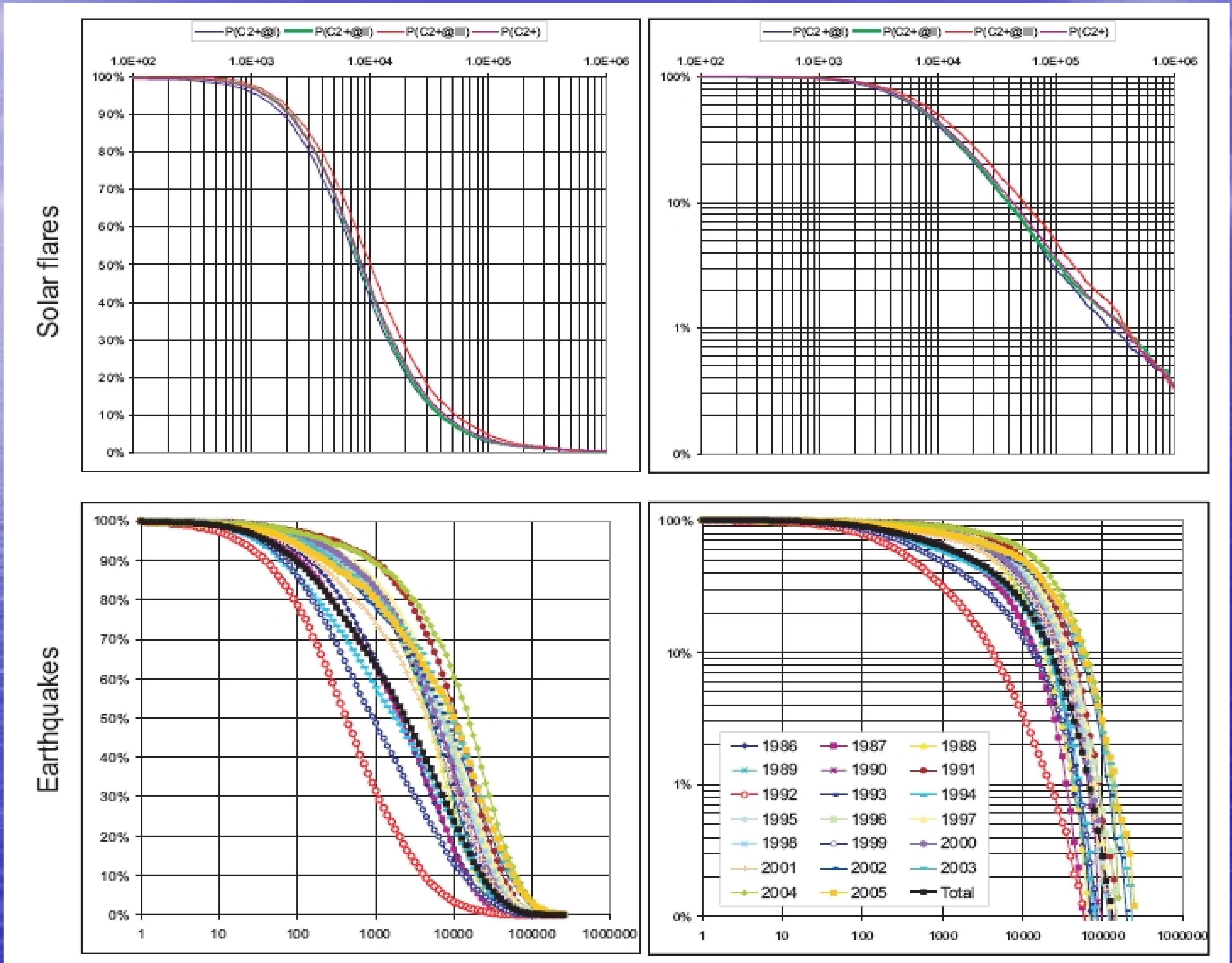

Inter-event time distributions in activity spots

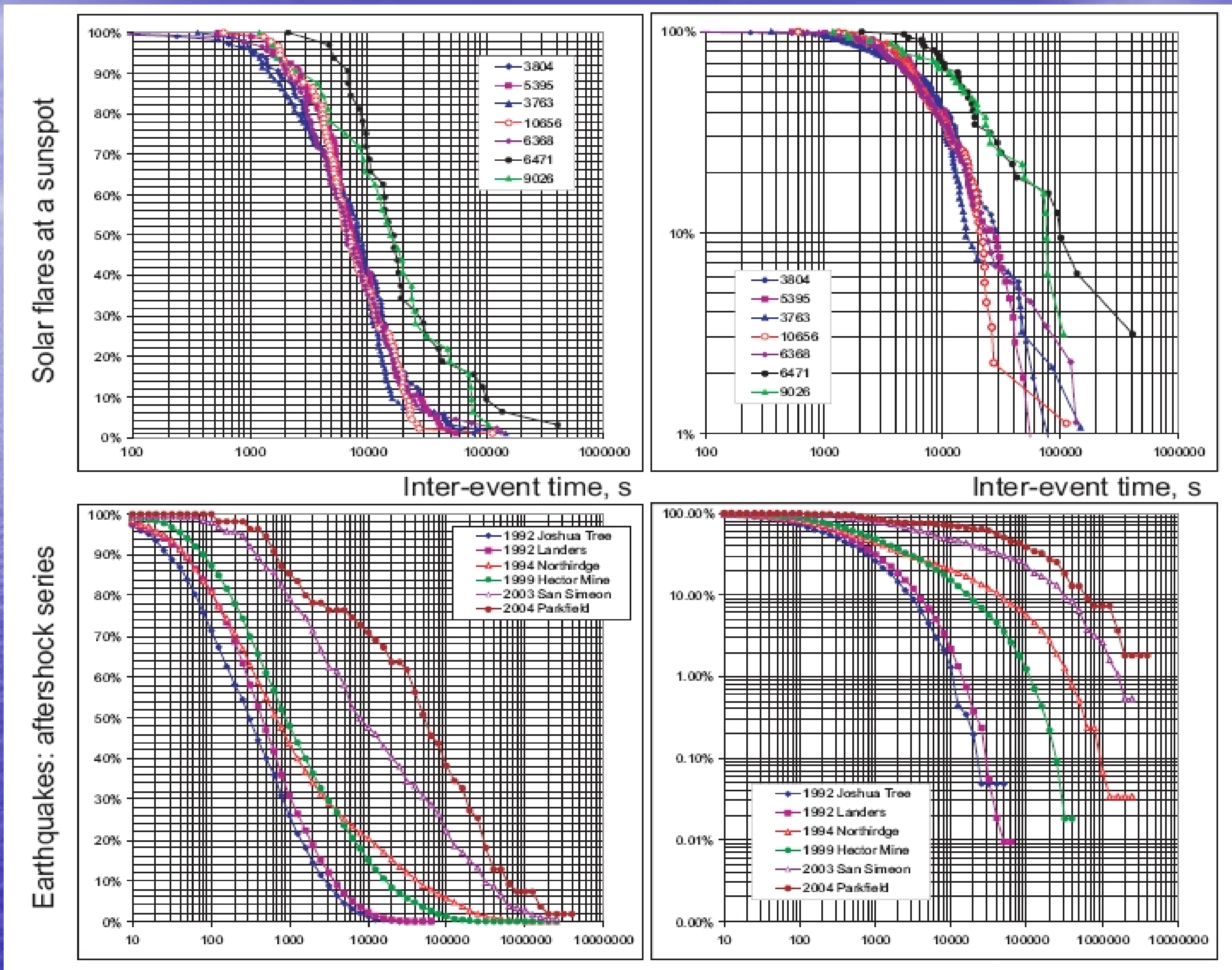

Inter-event time distributions

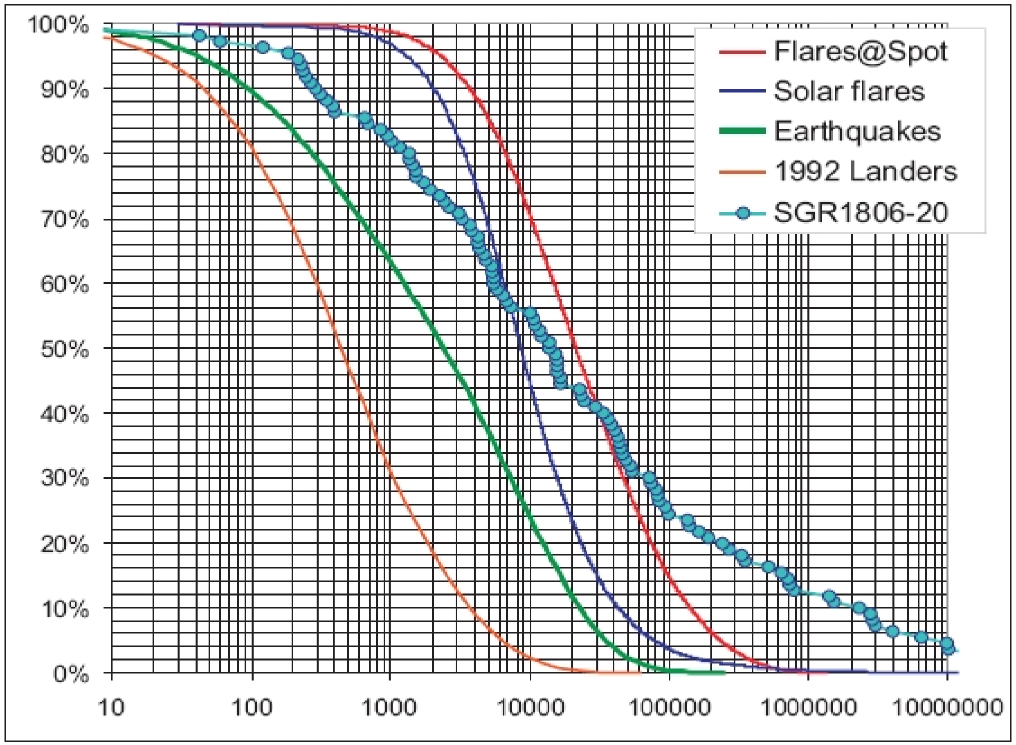

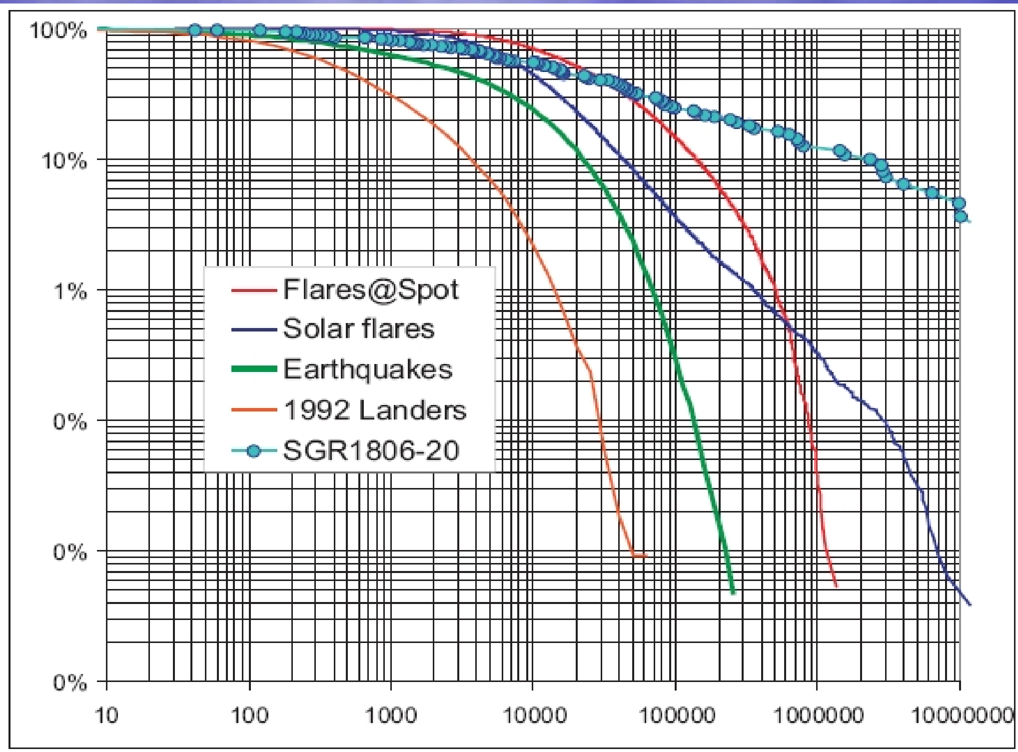

- The inter-event time distribution of soft γ-rays flashes produced by star-quakes on the neutron star 1806-20 is also shown (light blue circles). Energy released in a single event up to 10^{46} erg. (Kossobokov et al. 2000).

SGR1806-20 sequence

Soft-Gamma-Repeater 1806-20 is the source in Sagittarius, from which more than a hundred X-ray pulsations have been detected. Its location on the sky (1806-20 refer to celestial coordinates: 18 degrees 06 minutes right ascension, -20 degrees declination) is near the Galactic center, which is 25,000 light years away.

The energy of one burst varies from $1.4 \cdot 10^{40}$ erg to $5.3 \cdot 10^{41}$ erg (the largest earthquakes release about 10^{26} erg).

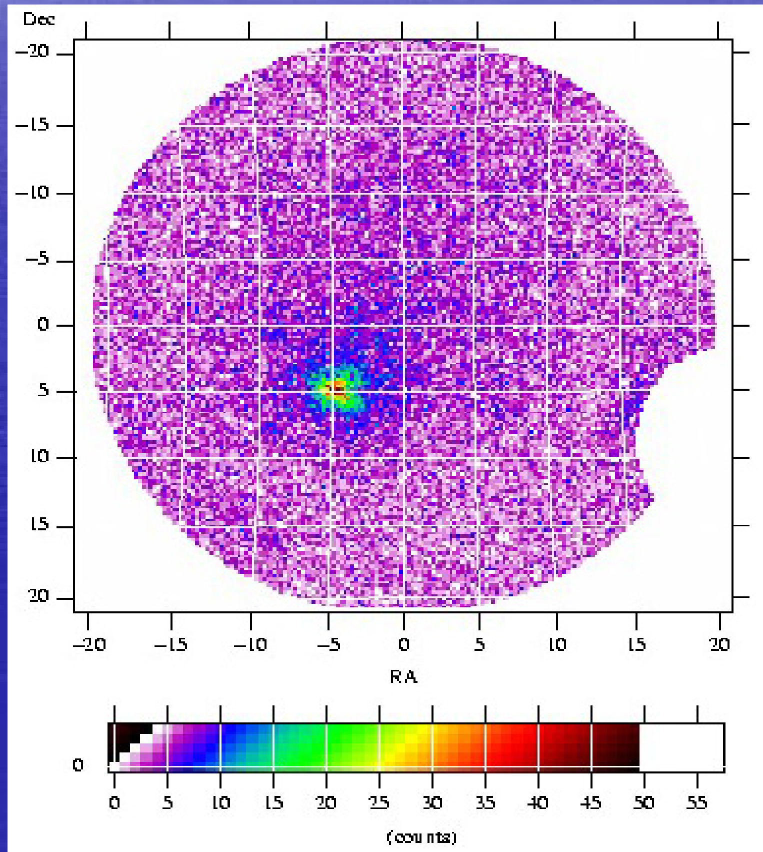

Common general features

A fundamental property of multiple fracturing is the power-law distribution of energy $\log_{10}N(E) = a + b\cdot\log_{10}E$

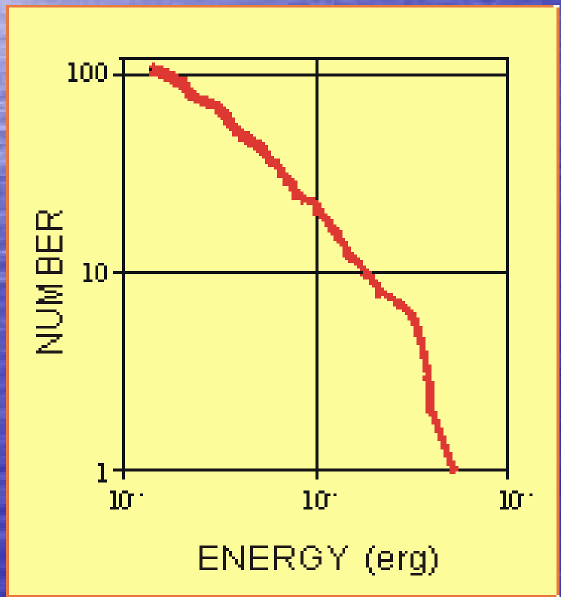

(Gutenberg-Richter relation)

Symptoms of transition to the main rupture

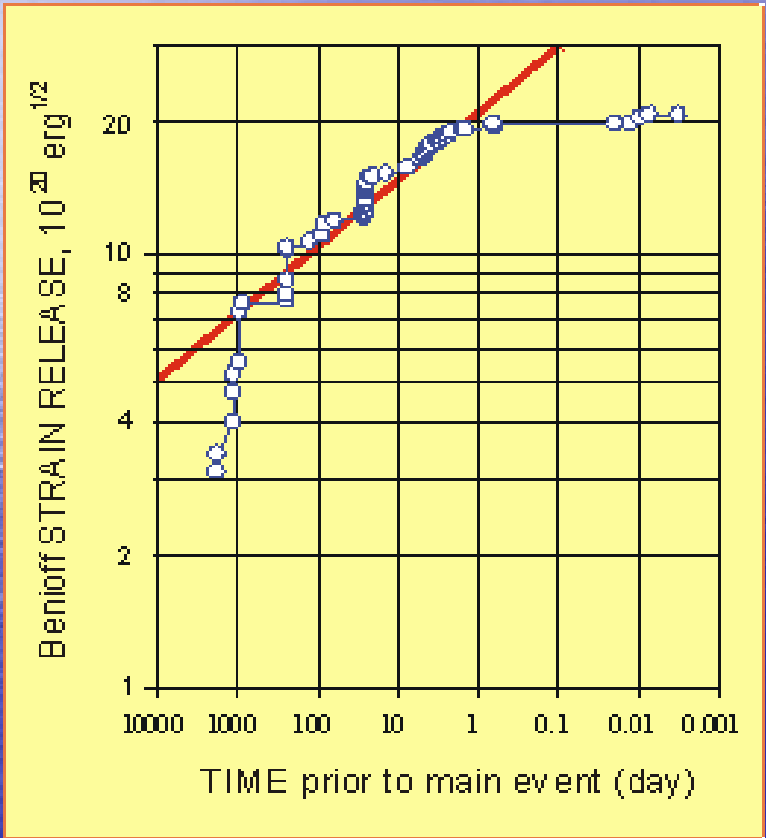

- Escalation of fracturing lasting nearly 1000 days and culminated with the largest starquake on November 16
- The power-law increase of activity, e.g. Benioff strain release $\varepsilon(t)$, with a possible trace of the four log-periodic oscillations.

Seismic premonitory patterns

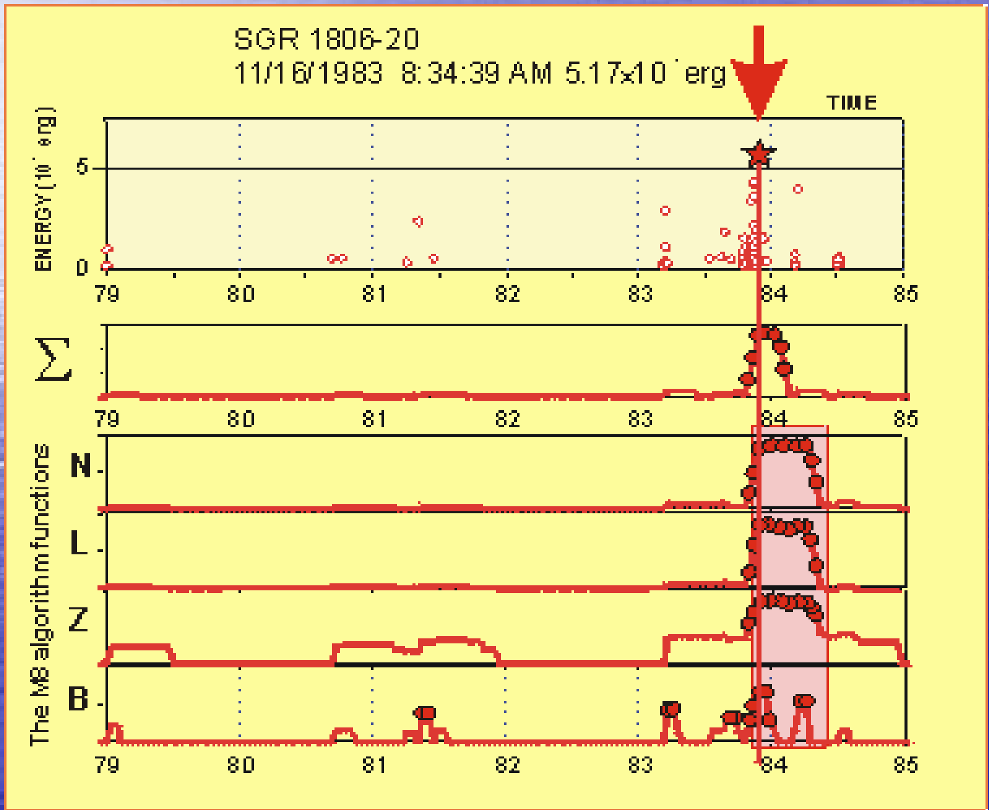

- Pattern $\Sigma \sim E^{2/3}$ *Keilis-Borok & Malinovskaya, 1964*
- Pattern B *Keilis-Borok, Knopoff & Rotwain, 1980*
- M8 algorithm *Keilis-Borok & Kossobokov, 1990*

Similarity of starquakes and earthquakes

Qualitative so far

- Gutenberg-Richter relation
- Premonitory changes
- Decay of "aftershocks"
  - – Omori power-law

Starquakes evidence drastic expansion of the Realm of Multiple Fracturing previously observed from the lithosphere of the Earth to laboratory samples

Kossobokov, Keilis-Borok & Cheng, 2000

Inter-event time distributions

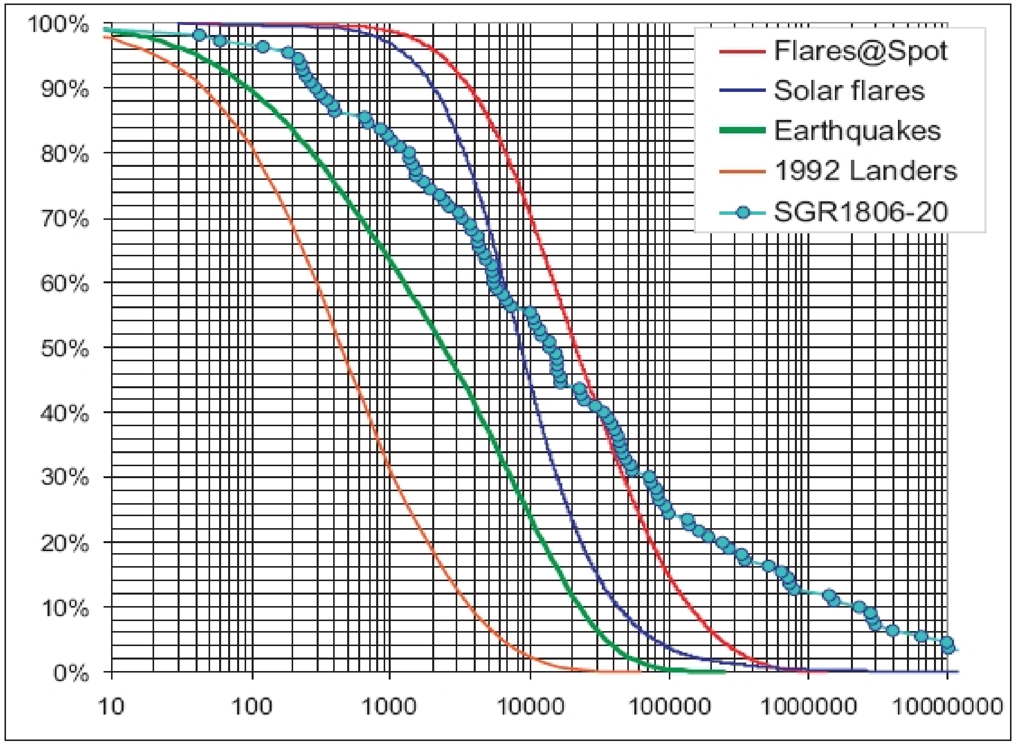

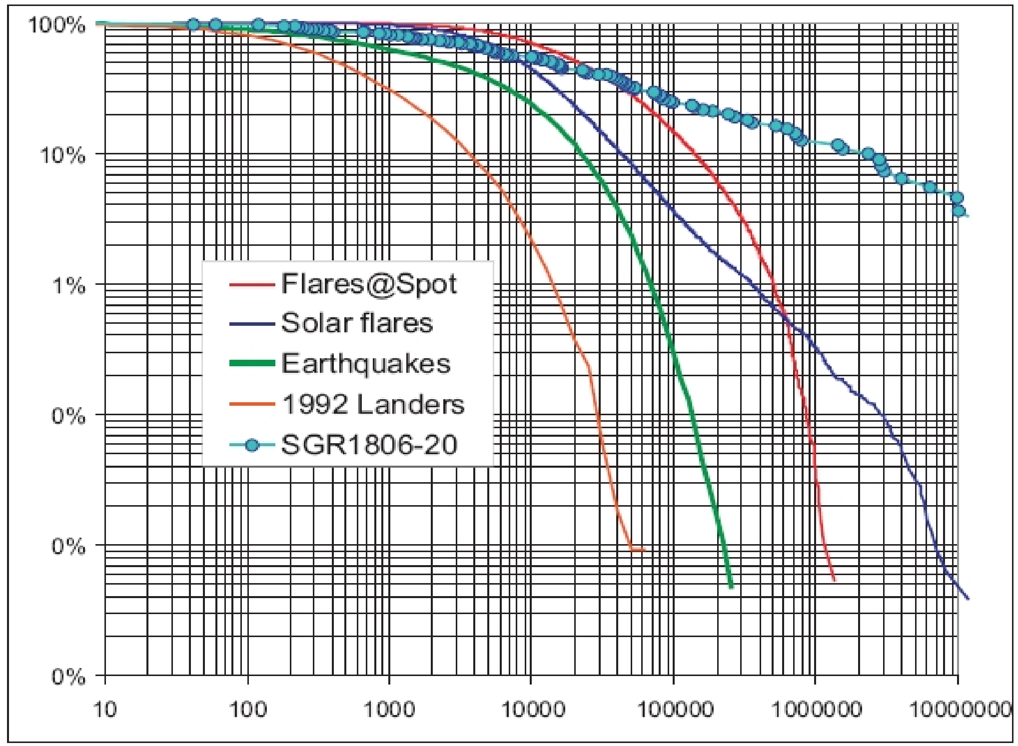

- The distributions show significant differences
- We calculated the minimum values of K-S statistic for all the couples of distributions over all rescaling fits of the type $P'(\Delta t)=P(C\,\Delta t^{\alpha})$, with C and α fitting constants

The K-S statistic

The two sample Kolmogoroff-Smirnoff statistic $\lambda_{K\text{-}S}$ is defined as

$$\lambda_{K\text{-}S}(D,n,m) = [nm/(n+m)]^{1/2} D$$

where $D = \max |P_{1,n}(\Delta t) - P_{2,m}(\Delta t)|$ is the maximum value of the absolute difference between the cumulative distributions $P_{1,n}(\Delta t)$ and $P_{2,m}(\Delta t)$ of the two samples, whose sizes are n and m respectively.

This test has the advantage of making no assumptions about the distribution of data. Moreover, it is widely accepted to be one of the most useful and general nonparametric methods for comparing two samples, as it is sensitive to differences in both location and shape of the empirical cumulative distribution functions of the two samples.

Inter-event time distributions:

The Kolmogoroff-Smirnoff two-sample criterion

	Flares	Flares at spot	SCSN	Landers	SGR1806-20
Flares	32076	3.435	8.648	2.071	0.636
Flares at spot	100 %	18878	5.898	1.669	0.434
SCSN	100 %	100 %	87688	3.726	1.435
Landers	99.96%	99.26%	100 %	10706	0.47
SGR1806-20	19.13%	0.92%	96.77%	2.24%	110

- The results indicate that the distributions cannot be rescaled onto the same curve (confidence level > 99%)
- Only the association of the starquake distribution (by far the smallest sample, 111 events) with all flares, flares at an activity spot, and Landers event cannot be rejected

Conclusions

- The statistics of inter-event times between earthquakes and solar flares show different scaling.
- Even the same phenomenon when observed in different periods or at different spots of activity show different scaling. This difference were found in our analysis both for earthquakes and solar flares
- In particular, the observed inter-event time distributions of different phenomena show a wide spectrum of scaling and cannot be rescaled onto a single curve
- Even if some statistical analogies are present (e.g. power laws of different characteristics), which could be related to common characteristics of impulsive energy release processes in critical nonlinear systems, our results do not support the presence of "universality"

Buyers Beware!

“Hierarchical evidence is a house of cards.

Pull out your primary assumption, and everything gets shaky.”

Regional Earthquake Likelihood Models: A realm on shaky grounds?

Likelihood scoring is one of the delicate tools of Statistics, which could be worthless or even misleading when inappropriate probability models are used. This is a basic loophole for a misuse of likelihood as well as other statistical methods on practice. The flaw could be avoided by an accurate verification of generic probability models on the empirical data. It is not an easy task in the frames of the Regional Earthquake Likelihood Models (RELM) methodology, which neither defines the forecast precision nor allows a means to judge the ultimate success or failure in specific cases. Hopefully, the RELM group realizes the problem and its members do their best to close the hole with an adequate, data supported choice.

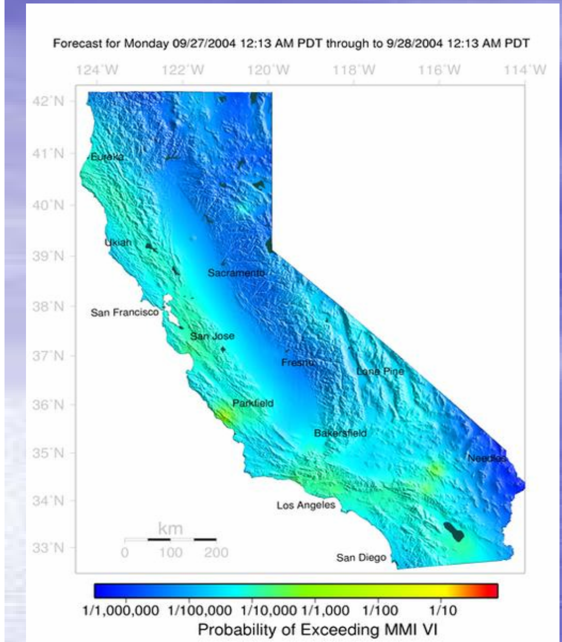

Regretfully, this is not the case with the erroneous choice of Gerstenberger et al., who started the public web site with forecasts of expected ground shaking for `tomorrow' (*Nature* 435, 19 May 2005).

Gerstenberger et al. **HAVE INVERTED THE CRITICAL EVIDENCE OF THEIR STUDY,** i.e., the 15 years of recent seismic record accumulated just in one key figure, which suggests rejecting with confidence above 97% "the generic California clustering model" used in automatic calculations.

Gerstenberger, M. C., Wiemer, S., Jones, L. M. & Reasenberg, P. A. Real-time forecasts of tomorrow's earthquakes in California. *Nature* **435**, 328-331 (19 May 2005)

Schorlemmer, D., Gerstenberger, M., Wiemer, S. & Jackson D. Earthquake Likelihood Model Testing (manuscript in preparation, February 7, 2005)

LETTERS NATURE|Vol 435|19 May 2005

Figure 3 | Calculated and observed rates of events $M \geq 4$ in 24-hour intervals following mainshocks occurring between 1988 and 2002 in southern California. Dashed lines show the rates forecasted by the generic California clustering model (without cascades) for the mainshock magnitude (M) shown. For this test a simple circular aftershock zone implementation (solid lines) gives the observed rates of $M \geq 4.0$ aftershocks following all mainshocks with magnitude within 0.5 units of M. The aftershock zones are defined as the areas within one rupture length of the mainshock epicentre.

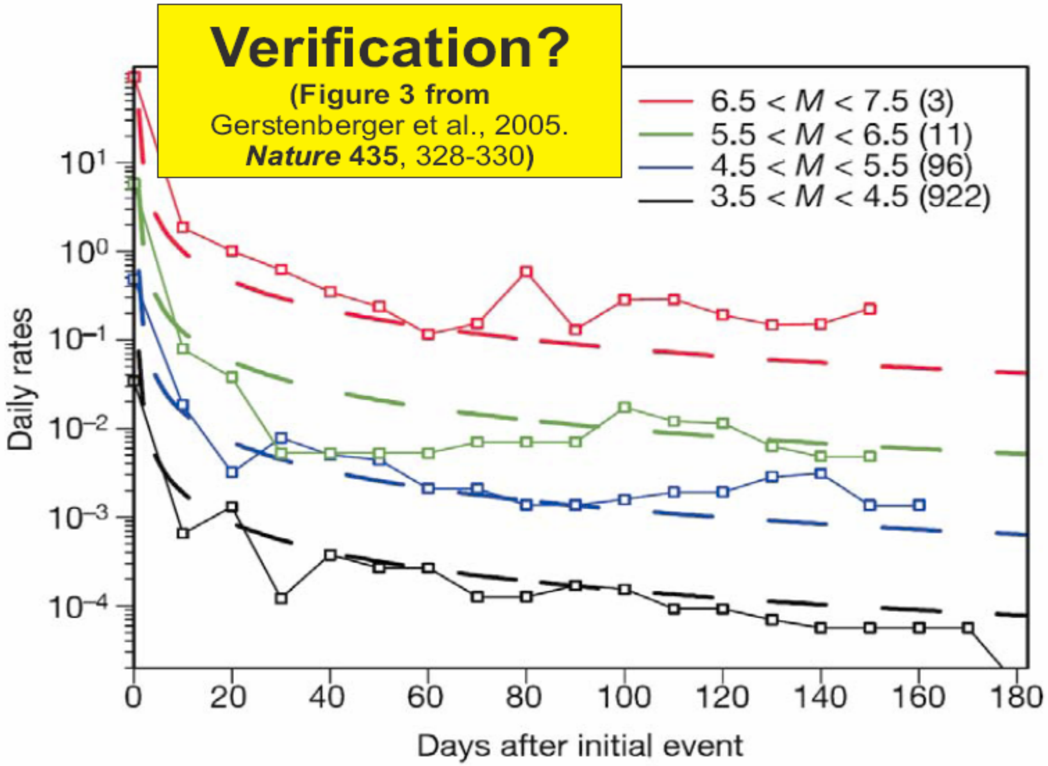

Soliciting misuse of Statistics?

"As a first test, we verified that the generic clustering model describes the average clustering activity of California reasonably well. Using data from 1988−2002, after the period used to initially develop the model and thus independent data, we compute the average daily rate of events following an earthquake of a given size (Fig. 3)."

Calculated and observed rates of events $M \geq 4$ in 24-hour intervals following mainshocks occurring between 1988 and 2002 in southern California.

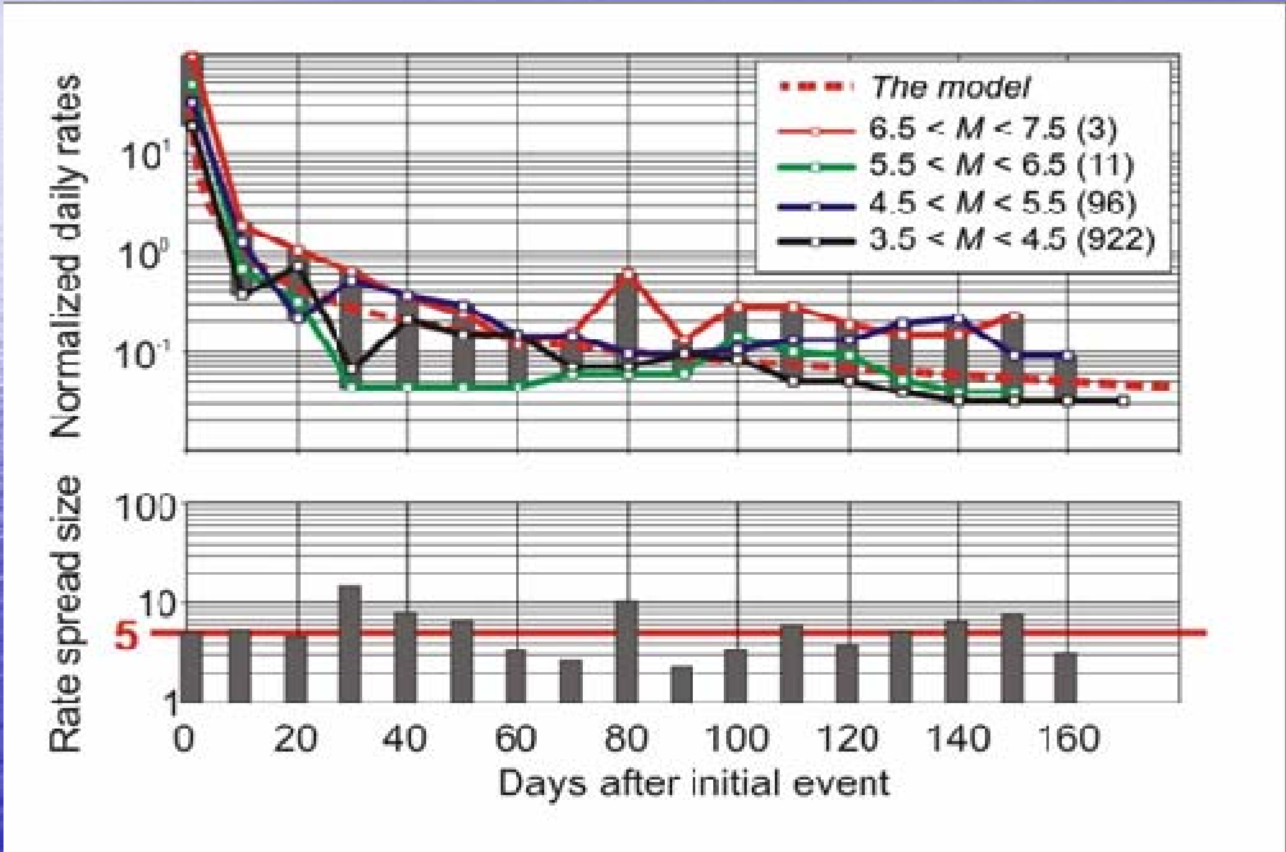

Dashed line shows the rate forecasted by the generic California clustering model for the initial mainshock of magnitude $6.5 < M < 7.5$; solid lines display the observed rates of $M \geq 4$ aftershocks following all mainshocks with magnitude within 0.5 units of M, normalized to the rate of the mainshock of magnitude $6.5 < M < 7.5$. Grey bars stretch from the minimal to the maximal value of the observed rates; their size is about a factor of 5.

Analyzing the figure by means of the well-known Kolmogoroff-Smirnoff criterion, an experimentalist would be led to reject the hypothesis that the random variable "Time after initial event" in different magnitude ranges of the initial event has the same statistical distribution.

Proof: Normalised by condition that the total integral of the p.d.f. (probability density function) increments equals 1, each of the four plots provides the minimum of positive p.d.f. increments, which are by definition either 1/N or its integer multiple (e.g., 2/N, 3/N, etc.). These are about 0.0012, 0.0008, 0.0025, and 0.0015, which values imply the sample sizes about 846, 1250, 401, and 665 or integer multiples of these values. The probability of a smaller value of the Kolmogoroff-Smirnoff statistic D than that for the two samples used to plot the daily rates after $5.5 < M < 6.5$ (green plot in Figure 3) event and after $3.5 < M < 4.5$ (black plot) event (i.e., $D = 0.07 \cdot (N_1 N_2/(N_1+N_2))^{1/2} \geq 2.12$) is larger than 97%,
Therefore, the hypothesis that these two samples are drawn from the same distribution can be rejected at significance level of 0.03. ■

(A skilful experimentalist would easily recognize the sample size in the order of a thousand just from the range of the empirical distribution of rates, about three decimal orders, in Figure 3, while a skilful observer would grasp 922 that signifies the number of events about magnitude 4. Moreover, giving a look at Figure 3, he or she, even without any statistical testing, would say that the data does not support the model.)

USGS Web Site May Mislead Californians

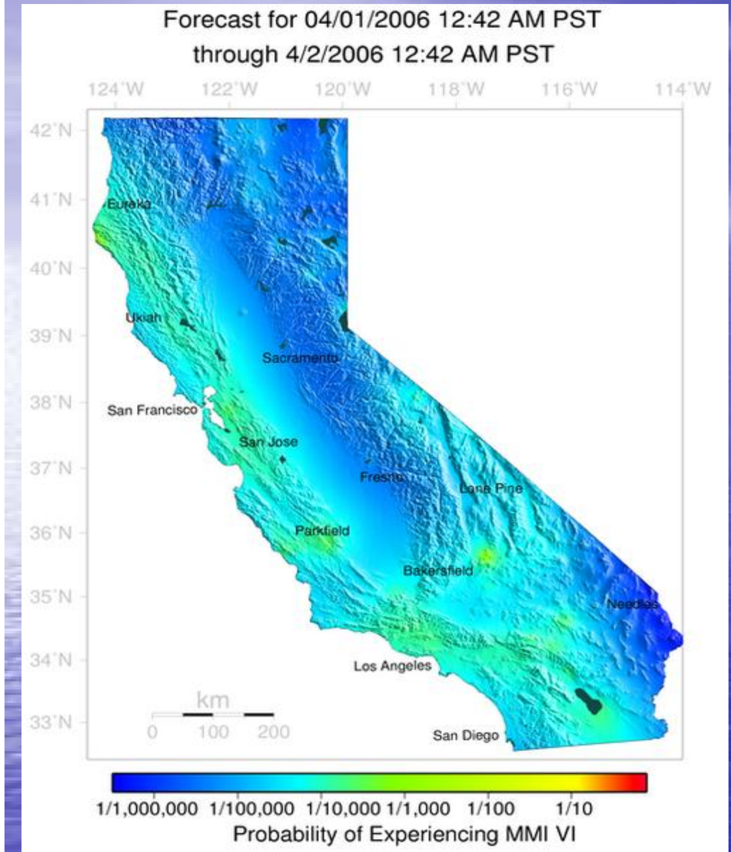

Since the time of *Nature* published the work by Gerstenberger *et al* on May 19, 2005 -

(i) In the 769 days (to Jun 27, 2007) of the real-time forecasting the four earthquakes of Modified Mercalli intensity VI in California have occurred in the "sky blue" areas of the web-site's lowest-risk (about 1/10000 or less). These are the earthquakes on June 12, 2005 near Anza; June 16, 2005 near Yucaipa; April 1, 2006 near Paicines; and August 3, 2006 W of Glen Ellen (pasadena.wr.usgs.gov/shake/ca).

(ii) The extent of the observed areas of intensity VI for these events is by far less than the expected number of cells experiencing VI or greater shaking:
about 100 for the four areas in total
vs. about 617 expected for 769 days.

As we see, this should not surprise Californians…

Regretfully, USGS continues delivering to the public, emergency planners and the media, a forecast product, which is based on wrong assumptions, which violates the best-documented earthquake statistics in California, which accuracy was not investigated, and which forecasts were not tested in any rigorous way.

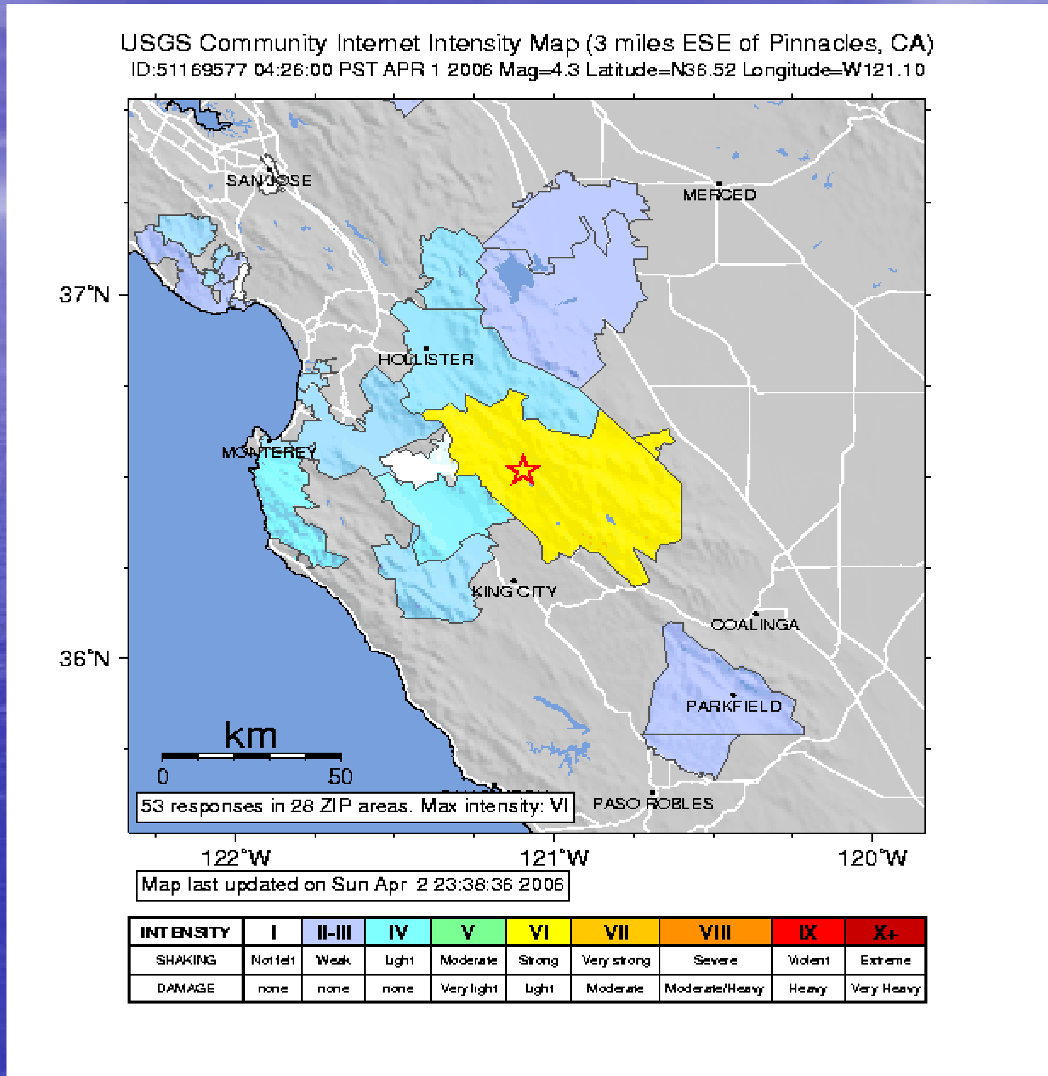
USGS Community Internet Intensity Map (3 miles ESE of Pinnacles, CA)
ID:51169577 04:26:00 PST APR 1 2006 Mag=4.3 Latitude=N36.52 Longitude=W121.10
SAN JOSE
MERCED
37°N
HOLLISTER
MONTEREY
KING CITY
COALINGA
36°N
PARKFIELD
km
0
50
53 responses in 28 ZIP areas. Max intensity: VI
PASO ROBLES
122°W
121°W
120°W
Map last updated on Sun Apr 2 23:38:36 2006
INTENSITY | I | II-III | IV | V | VI | VII | VIII | IX | X+
SHAKING | Not felt | Weak | Light | Moderate | Strong | Very strong | Severe | Violent | Extreme
DAMAGE | none | none | none | Very light | Light | Moderate | Moderate/Heavy | Heavy | Very Heavy

West Pacific short-term forecast

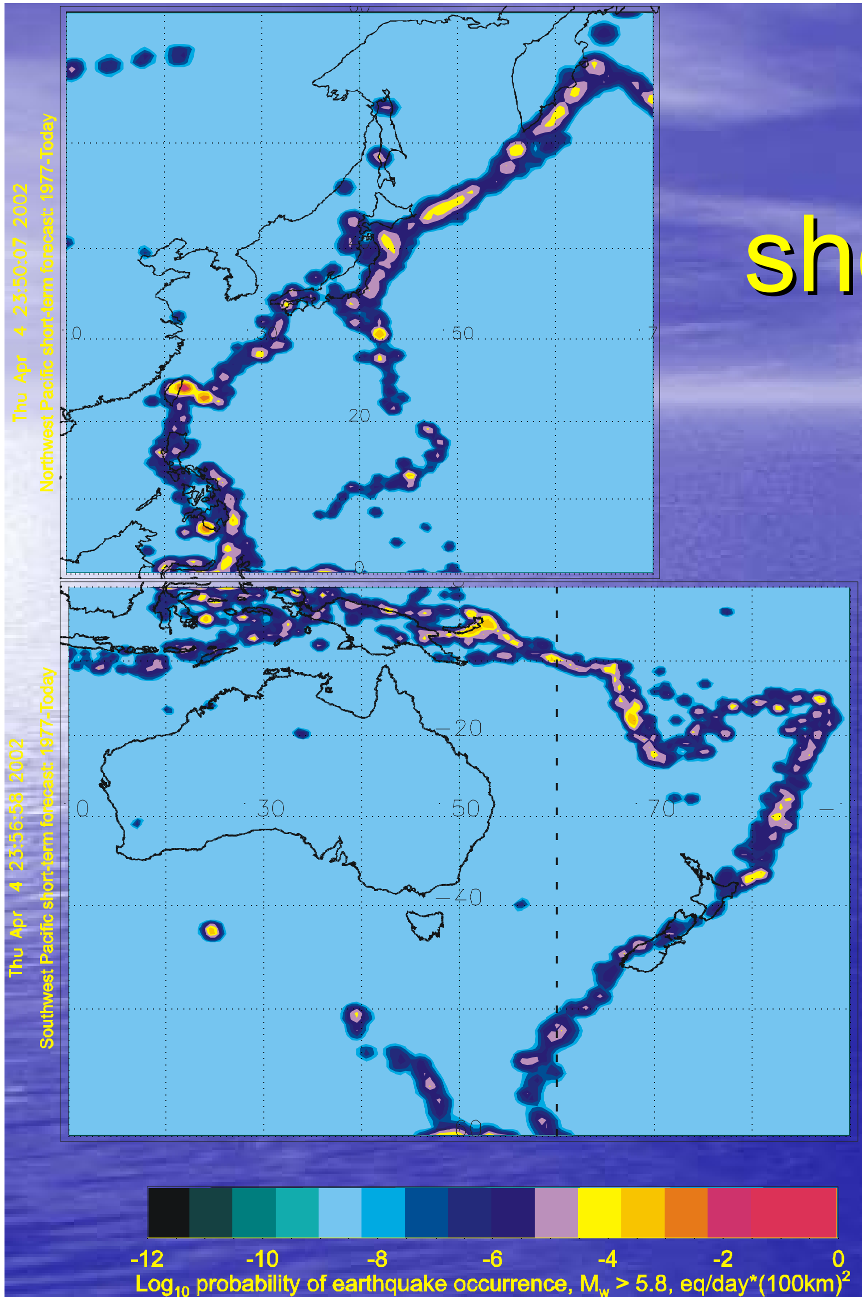

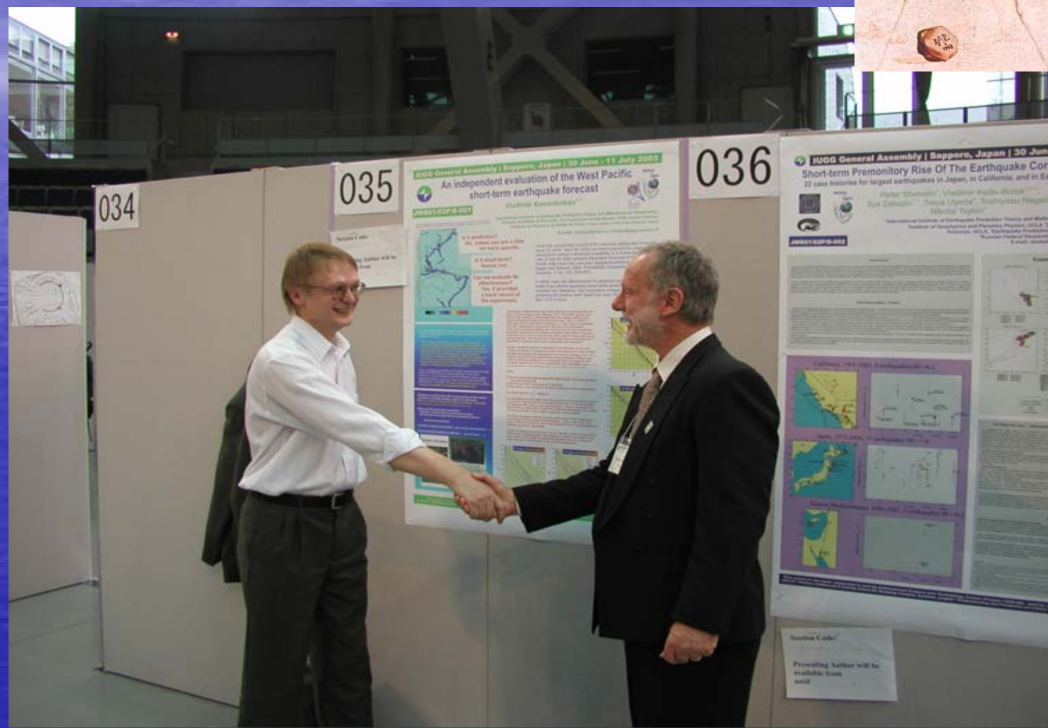

Jackson and Kagan "Testable earthquake forecasts for 1999", Seism. Res. Lett., 70, 393-403, 1999

Kagan and Jackson (2000) "Probabilistic forecasting of earthquakes", Geophys. J. Int., 143, 438-453

We have analyzed the predictions arising from setting a threshold probability or a threshold probability ratio on top the daily updated Short-term forecasts for NW and SW Pacific in April 2002 - September 2004 (*http://scec.ess.ucla.edu/~ykagan/predictions_index.html*; *Kagan and Jackson, 2000. Probabilistic forecasting of earthquakes, Geophys. J. Int., 143, 438-453*) and the catalog of earthquakes for the same period and have come to the following conclusion:

The predictions based on the Yan Y. Kagan and David D. Jackson forecasts are hardly better than random guessing, when main shocks are considered, and could be used for effective prediction of aftershocks only.

The conclusion is based on the prediction outcome achieved for 218 shallow (with depth less than 70 km) earthquakes of MwHRV = 5.8 or more. According to the definition from (*Keilis-Borok et al., 1980*), there are 67 aftershocks and 151 main shocks.

The territory of West Pacific short-term forecast is coarse-grained into cells, 0.5 by 0.5 degree each. Making a “bet” on a cell C, we pay n(C), which is the number of earthquakes from the sample catalog. Each target earthquake E defines the threshold value - p(E) (or p/P(E)) - being the value of short-term probability p (or the value of probability ratio p/P) determined in advance for the day of the earthquake.

In its turn the threshold defines the minimal cost of a bet required for successful prediction of the target earthquake, N(E), which is the sum of all bets n(C) over the union of cells with p equal or above p(E) (same for the ratio p/P). The track record of the experiment provides the set of bets {N(E)} associated with target earthquakes that happened.

Seismic Roulette

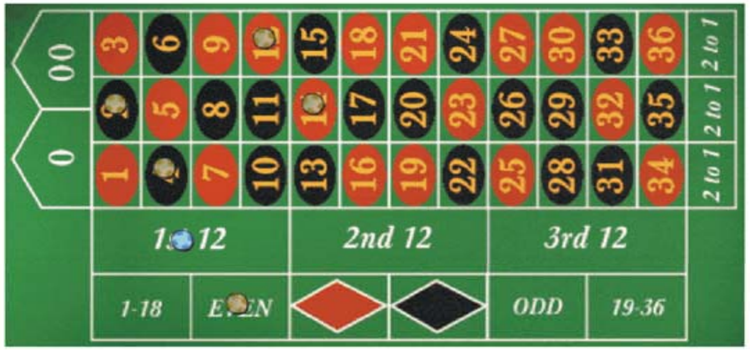

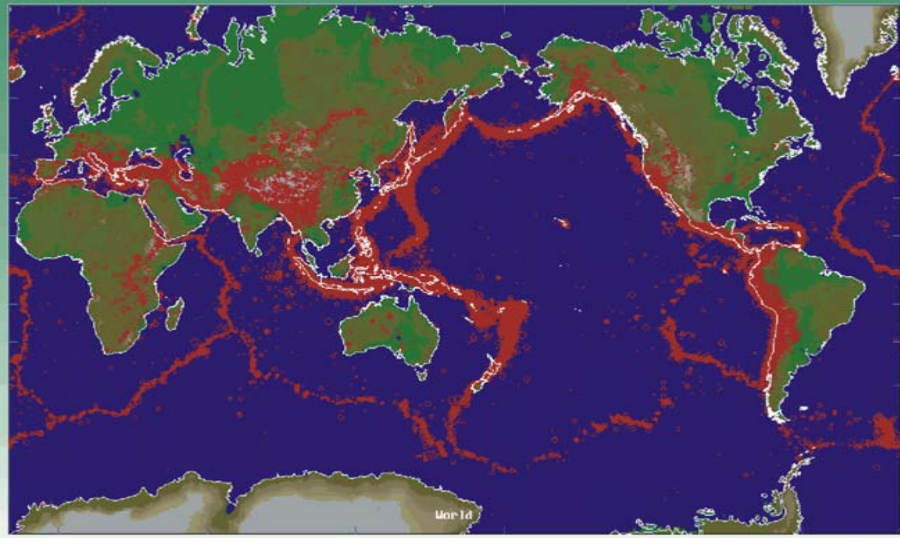

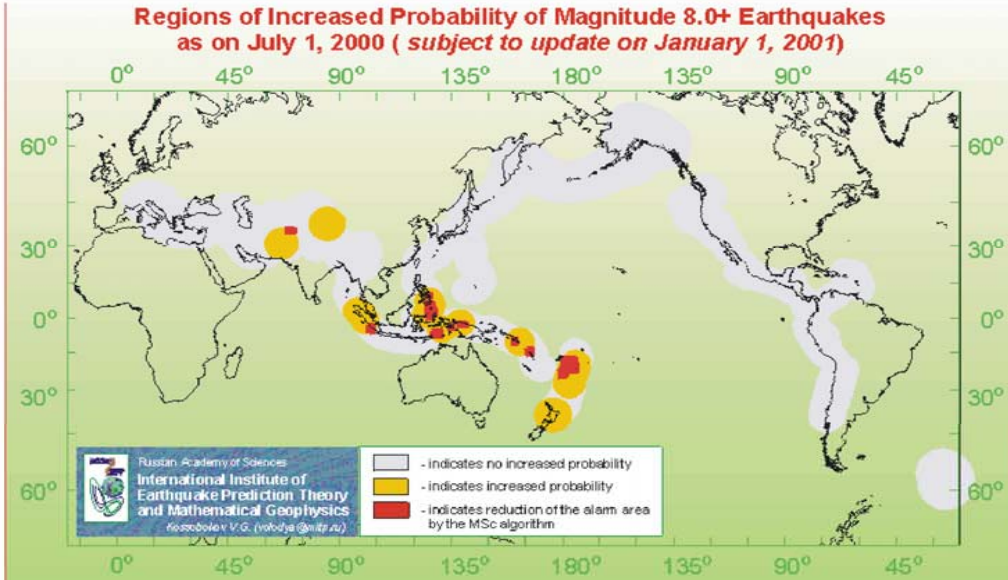

Seismic Roulette

Consider a roulette wheel with as many sectors as the number of events in a sample catalog, a sector per each event.

- Make your bet according to prediction: determine, which events are inside area of alarm, and put one chip in each of the corresponding sectors.
- Nature turns the wheel.
- If seismic roulette is not perfect…

then ***systematically*** you can win! ☺

and lose … ☹

If you are smart enough and your predictions are effective ------

the first will outscore the second! ☺ ☺ ☹ ☺ ☺ ☺ ☹ ☺ ☺ ☺

Denote μ being the bet sum normalized to the total sum of n(C) and ν being the number of failures-to-predict normalized to the total number of target earthquakes that happened in the course of testing. The ν vs. μ diagram characterize the effectiveness of the prediction method, e.g., random prediction performance is associated with the diagonal that connects "optimist's" {1,0} and "pessimist's" {0,1} strategies (*Molchan, G. M.. Earthquake Prediction as a Decision-making Problem, Pure Appl. Geophys., 149, 233-247, 1997*).

Given -

(1) the track record of the West Pacific short-term forecasts in the period from April 10, 2002 to September 13, 2004;

(2) the Harvard CMT catalog for the same period of time;

(3) the counts of n(C) based on the NEIC catalog of shallow earthquakes -

we plotted several ν vs. μ diagrams.

The two figures show the performance of predictions based on p or p/P in the test period from April 10, 2002 to September 13, 2004. The total of 218 earthquakes of magnitude Mw = 5.8 or more with the depth of 70 km or shallower occurred in the West Pacific. According to definition from (*Keilis-Borok et al., 1980*), 67 of them are aftershocks and 151 main shocks.

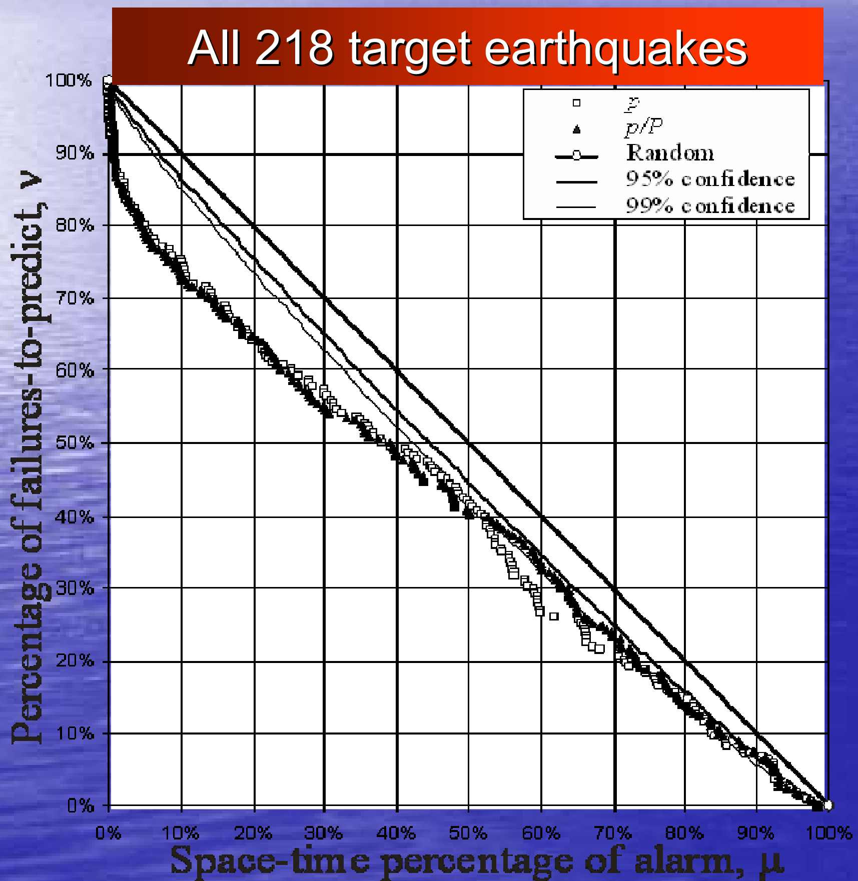

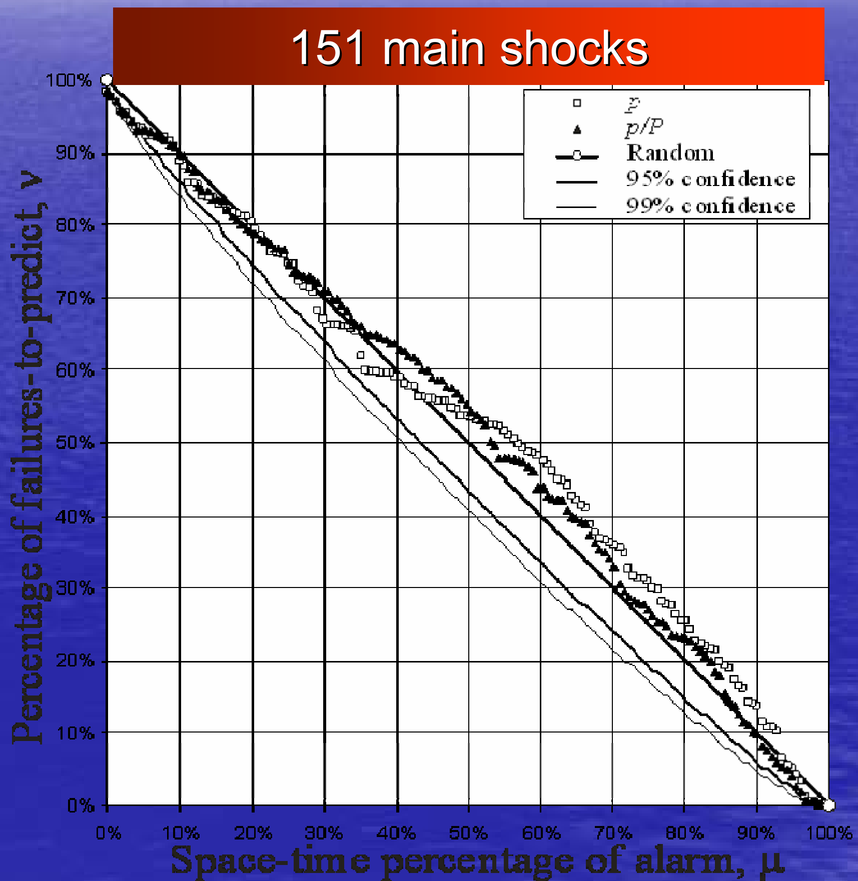

The outcome of an "absurd" prediction:

The percentage of the failures-to-predict ν versus the percentage of the alerted space-time volume μ: $\{\mu_p(E), \nu_p(E)\}$ and $\{\mu_{p/P}(E), \nu_{p/P}(E)\}$ generated by "prediction" of the 231 earthquakes with magnitude MwHRV ≥ 5.8 and depth ≳ 70 km in April 10, 1992-September 13, 1994 using the *p* and *p/P* maps computed for April 10, 2002-September 13, 2004.

"Delayed" 231 earthquakes

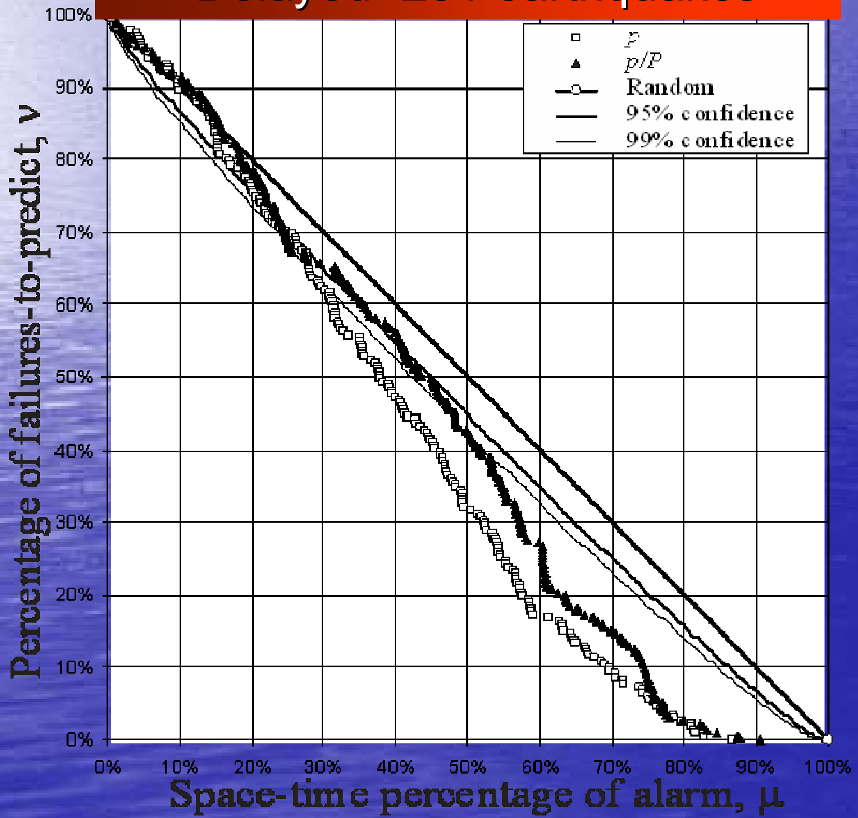

The observed deviation from the diagonal is about the same or larger than in the real-time applications.

Thus, we cannot reject random nature of the Jackson-Kagan "probabilistic" method and may conclude that (i) its effectiveness for predicting large earthquakes is doubtful, and (ii) the applicability of the underlying ETAS model is an ingrained bigotry.

Seismology is juvenile and its appropriate statistical tools to-date may have a "medieval flavor" for those who hurry up to apply a fuzzy language of a highly developed probability theory. To become "quantitatively probabilistic" earthquake forecasts/predictions must be defined with a scientific accuracy. Following the most popular objectivists' viewpoint on probability, we cannot claim "probabilities" adequate without a long series of "yes/no" forecast/prediction outcomes. Without "antiquated binary language" of "yes/no" certainty we cannot judge an outcome ("success/failure"), and, therefore, quantify objectively a forecast/prediction method performance.

Global warming: Models vs. Temperature

Data

THE FOLLOWING SOURCE IS ACKNOWLEDGED:

Klein Tank, A.M.G. and Coauthors, 2002. Daily dataset of 20th-century surface air temperature and precipitation series for the European Climate Assessment.
Int. J. of Climatol., 22, 1441-1453.
Data and metadata available at http://eca.knmi.nl

Source identifier, Date, daily Minimum and Maximum temperature in 0.1 °C, and quality code

"Hierarchical evidence is a house of cards.

Pull out your primary assumption, and everything gets shaky."

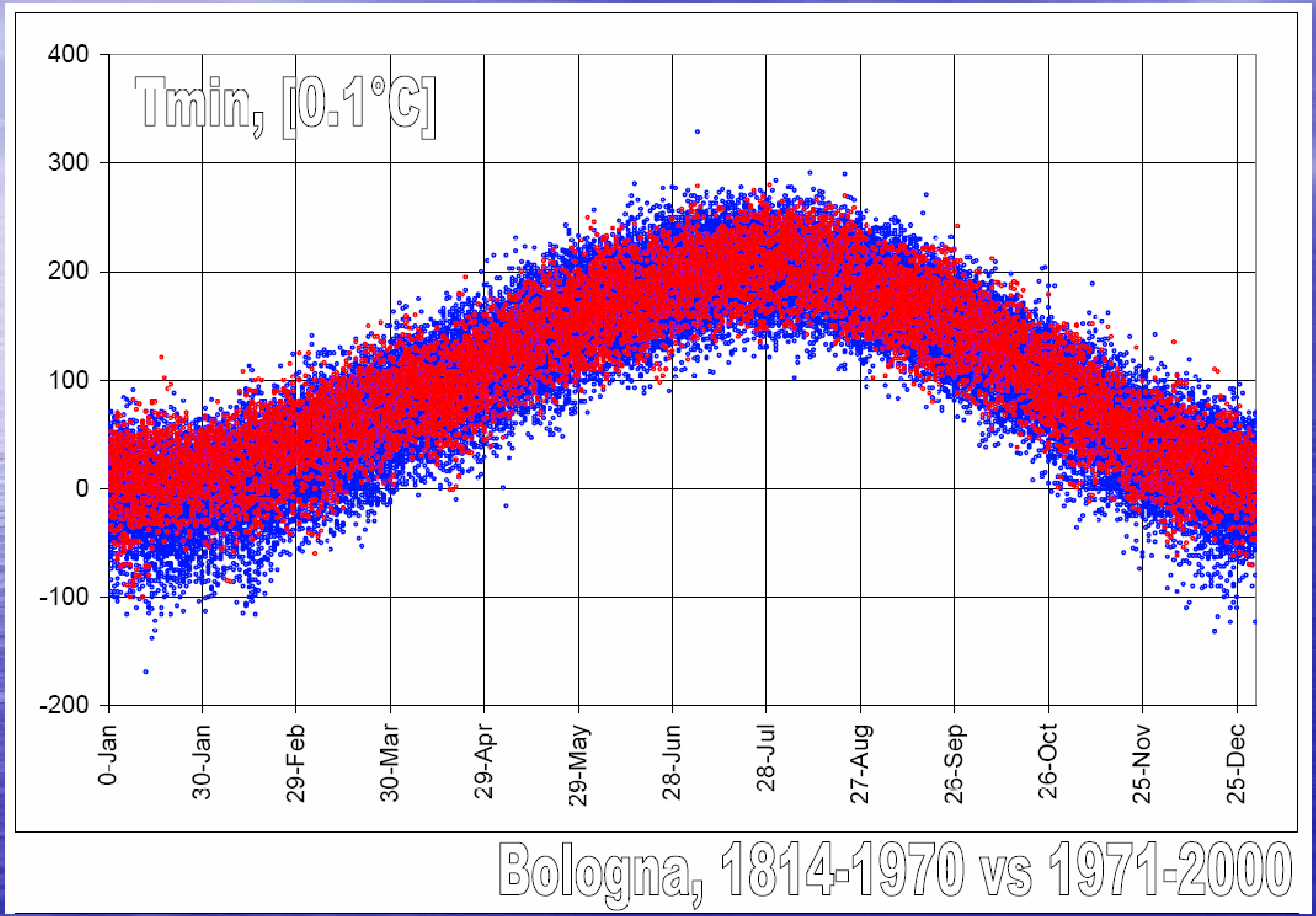
Tmin, [0.1°C]
400
300
200
100
0
-100
-200
0-Jan
30-Jan
29-Feb
30-Mar
29-Apr
29-May
28-Jun
28-Jul
27-Aug
26-Sep
26-Oct
25-Nov
25-Dec
Bologna, 1814-1970 vs 1971-2000

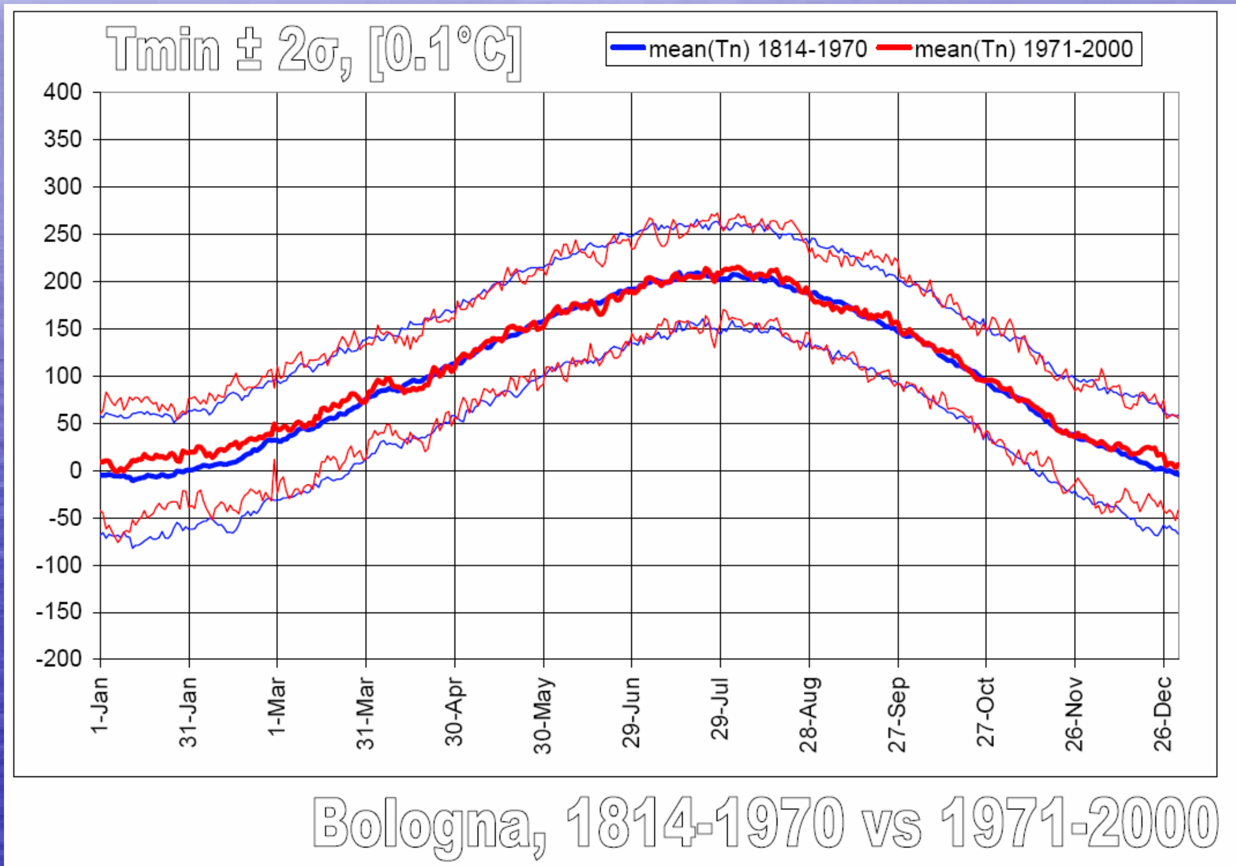
Tmin ± 2σ, [0.1°C]
mean(Tn) 1814-1970
mean(Tn) 1971-2000
400
350
300
250
200
150
100
50
0
-50
-100
-150
-200
1-Jan
31-Jan
1-Mar
31-Mar
30-Apr
30-May
29-Jun
29-Jul
28-Aug
27-Sep
27-Oct
26-Nov
26-Dec
Bologna, 1814-1970 vs 1971-2000

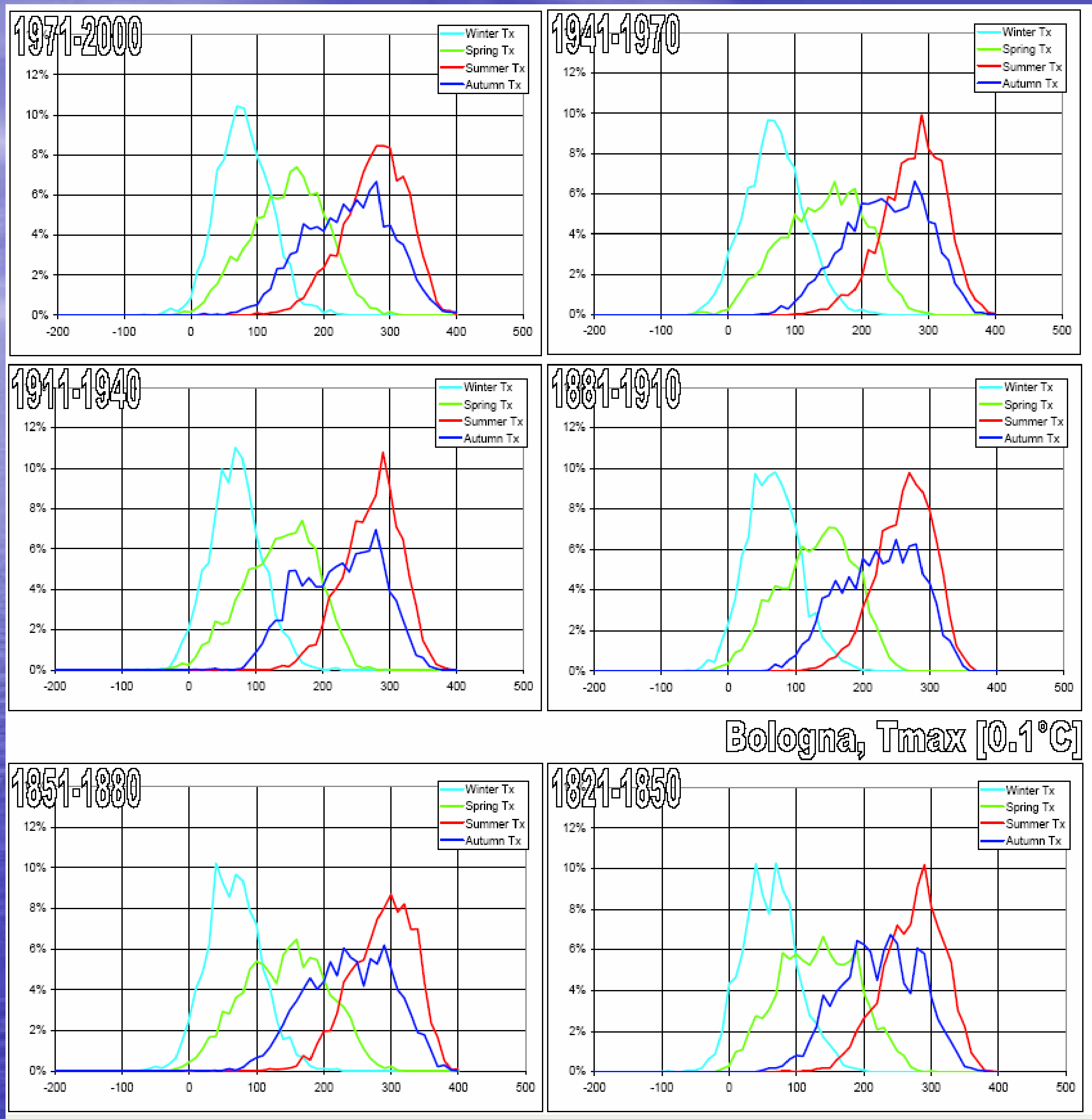
1971-2000
1941-1970
1911-1940
1881-1910
1851-1880
1821-1850
Winter Tx
Spring Tx
Summer Tx
Autumn Tx
Bologna, Tmax [0.1°C]

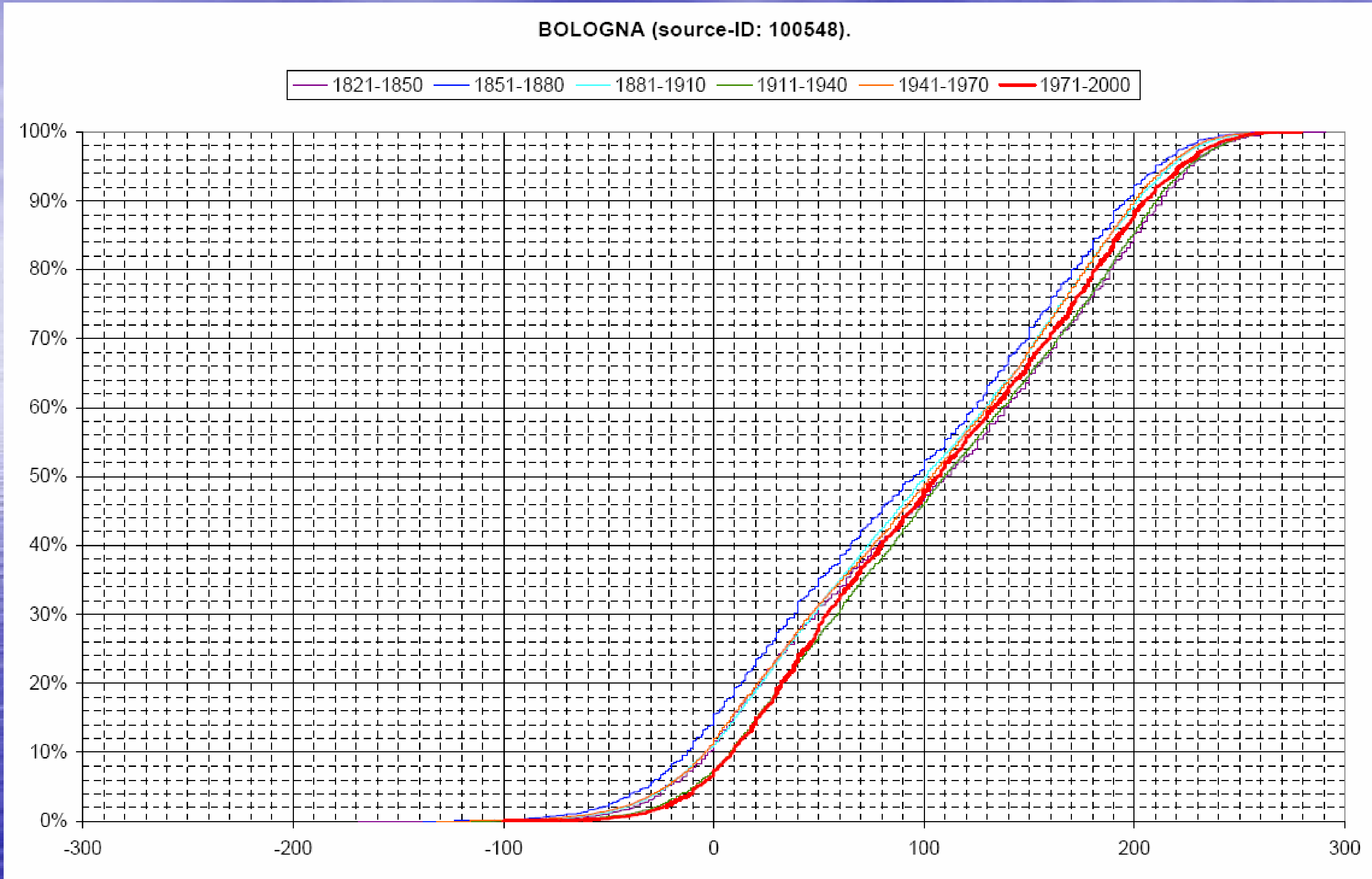
BOLOGNA (source-ID: 100548).
1821-1850
1851-1880
1881-1910
1911-1940
1941-1970
1971-2000
100%
90%
80%
70%
60%
50%
40%
30%
20%
10%
0%
-300
-200
-100
0
100
200
300

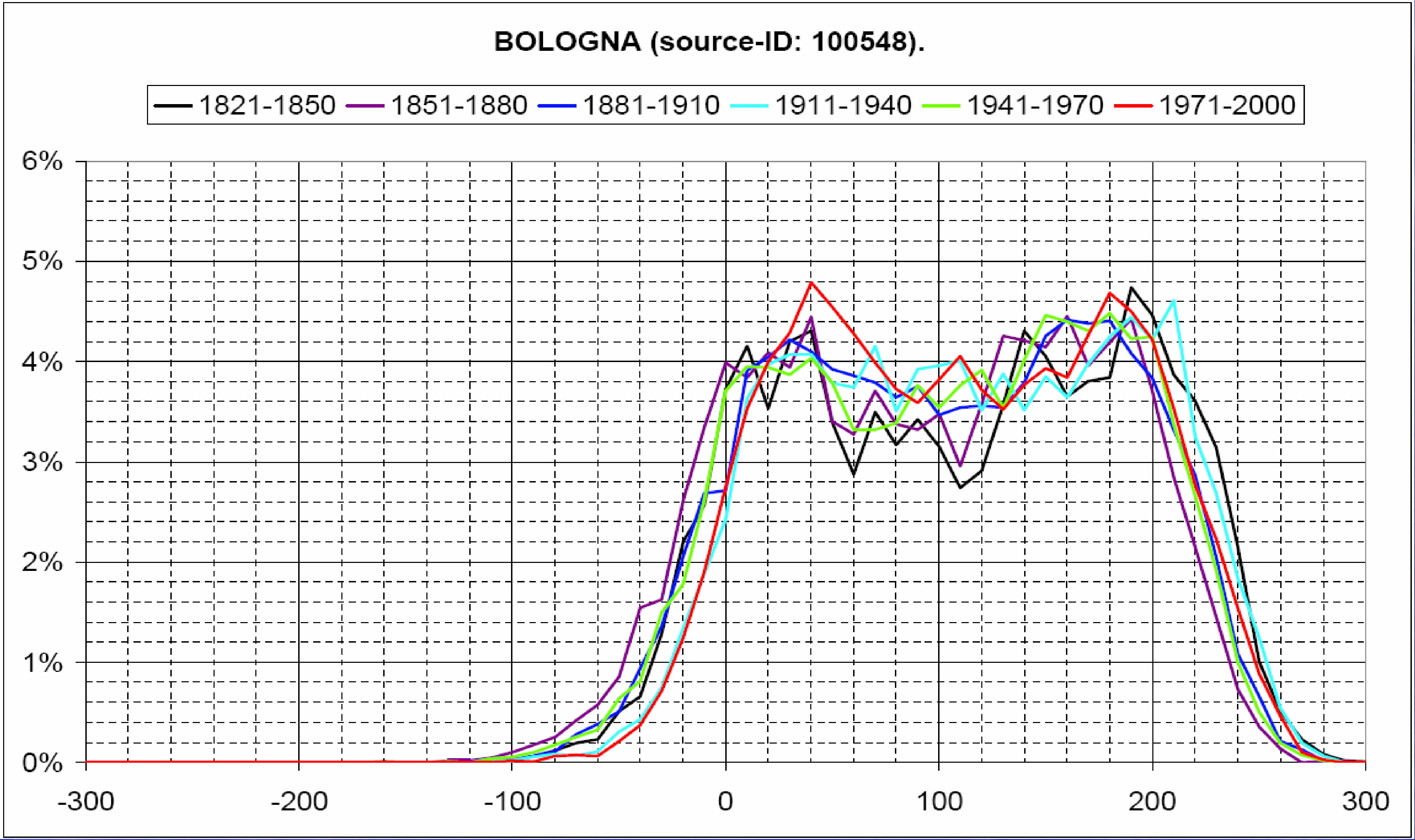
BOLOGNA (source-ID: 100548).
1821-1850
1851-1880
1881-1910
1911-1940
1941-1970
1971-2000
6%
5%
4%
3%
2%
1%
0%
-300
-200
-100
0
100
200
300

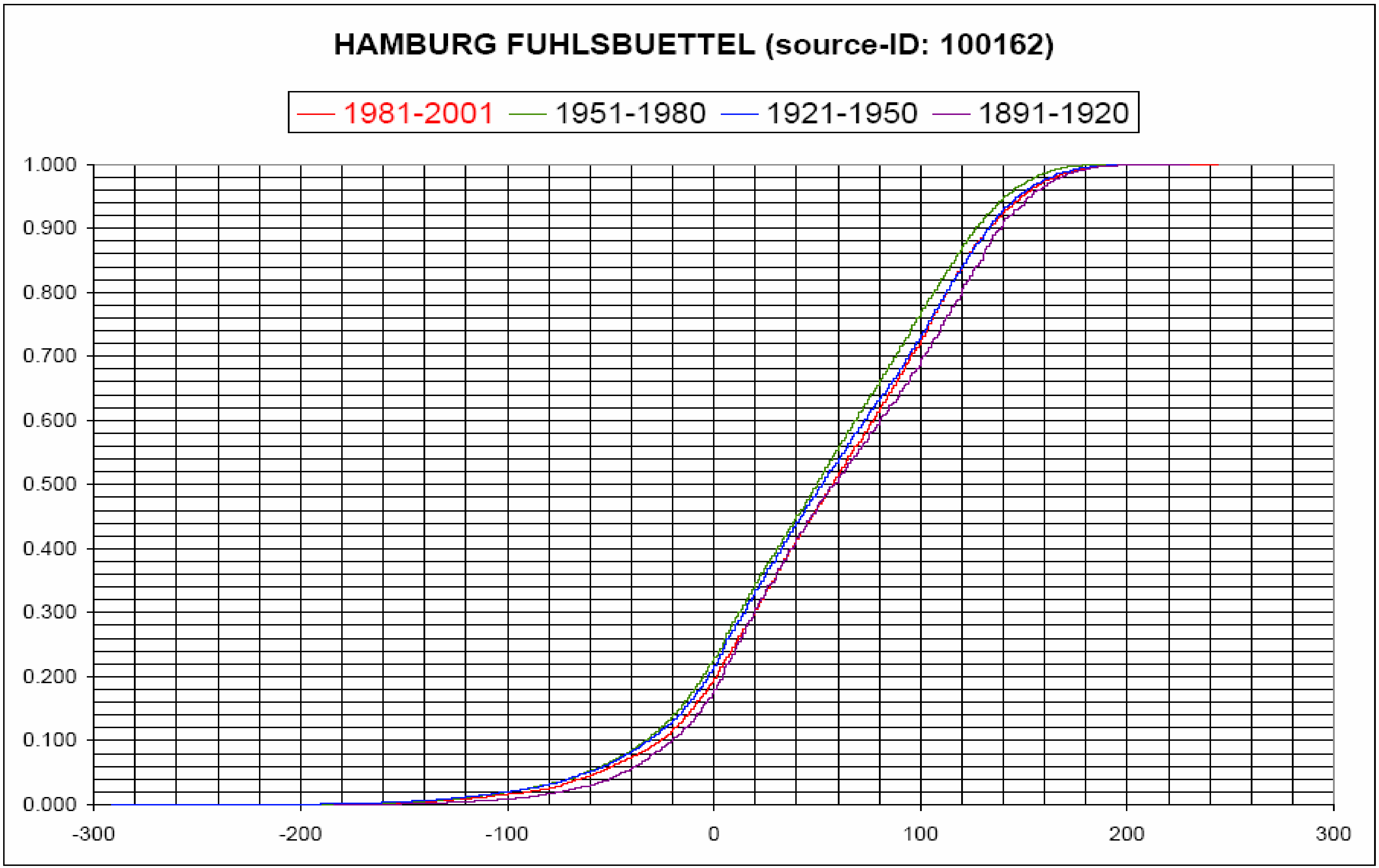
HAMBURG FUHLSBUETTEL (source-ID: 100162)
1981-2001
1951-1980
1921-1950
1891-1920
1.000
0.900
0.800
0.700
0.600
0.500
0.400
0.300
0.200
0.100
0.000
-300
-200
-100
0
100
200
300

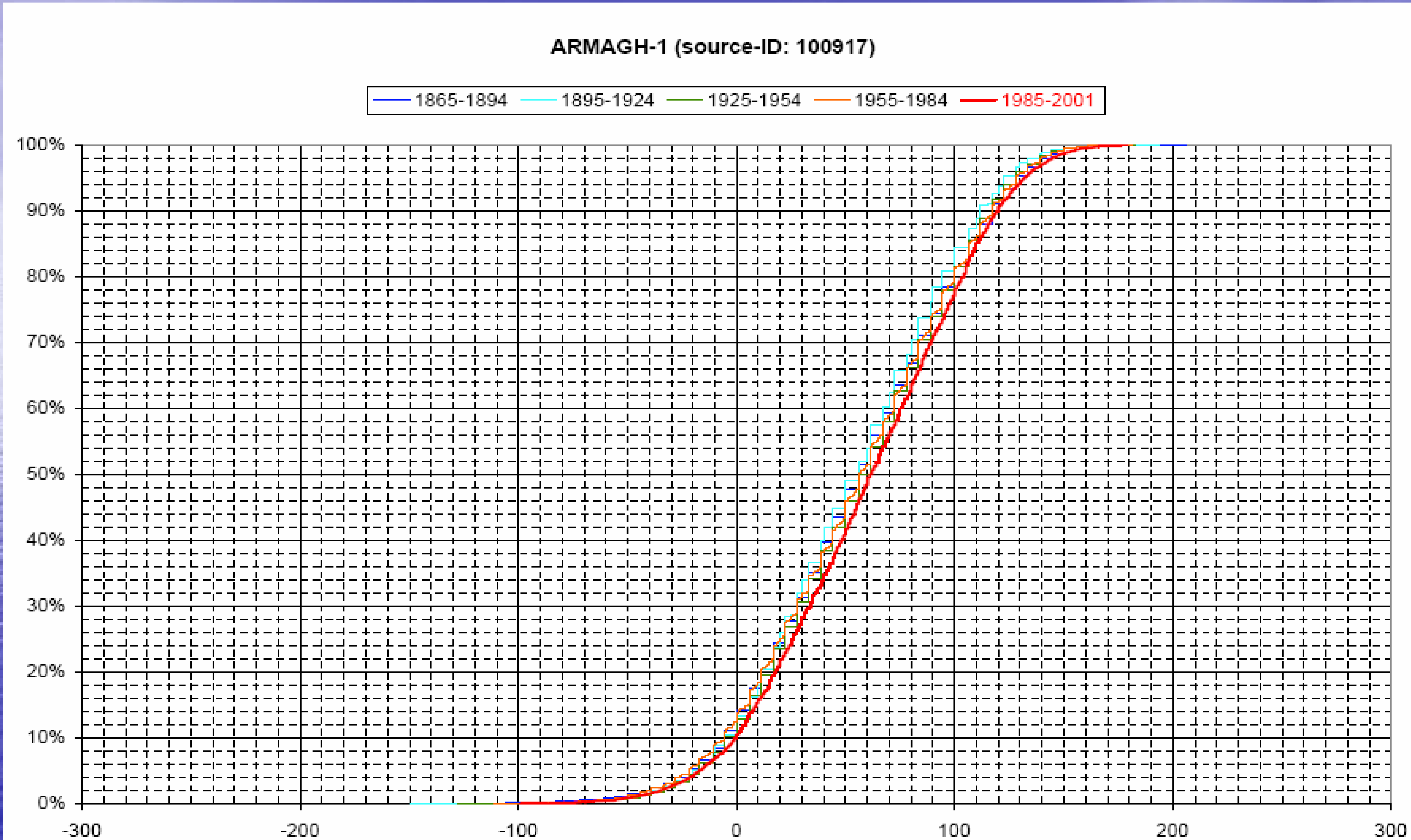
ARMAGH-1 (source-ID: 100917)
1865-1894
1895-1924
1925-1954
1955-1984
1985-2001
100%
90%
80%
70%
60%
50%
40%
30%
20%
10%
0%
-300
-200
-100
0
100
200
300

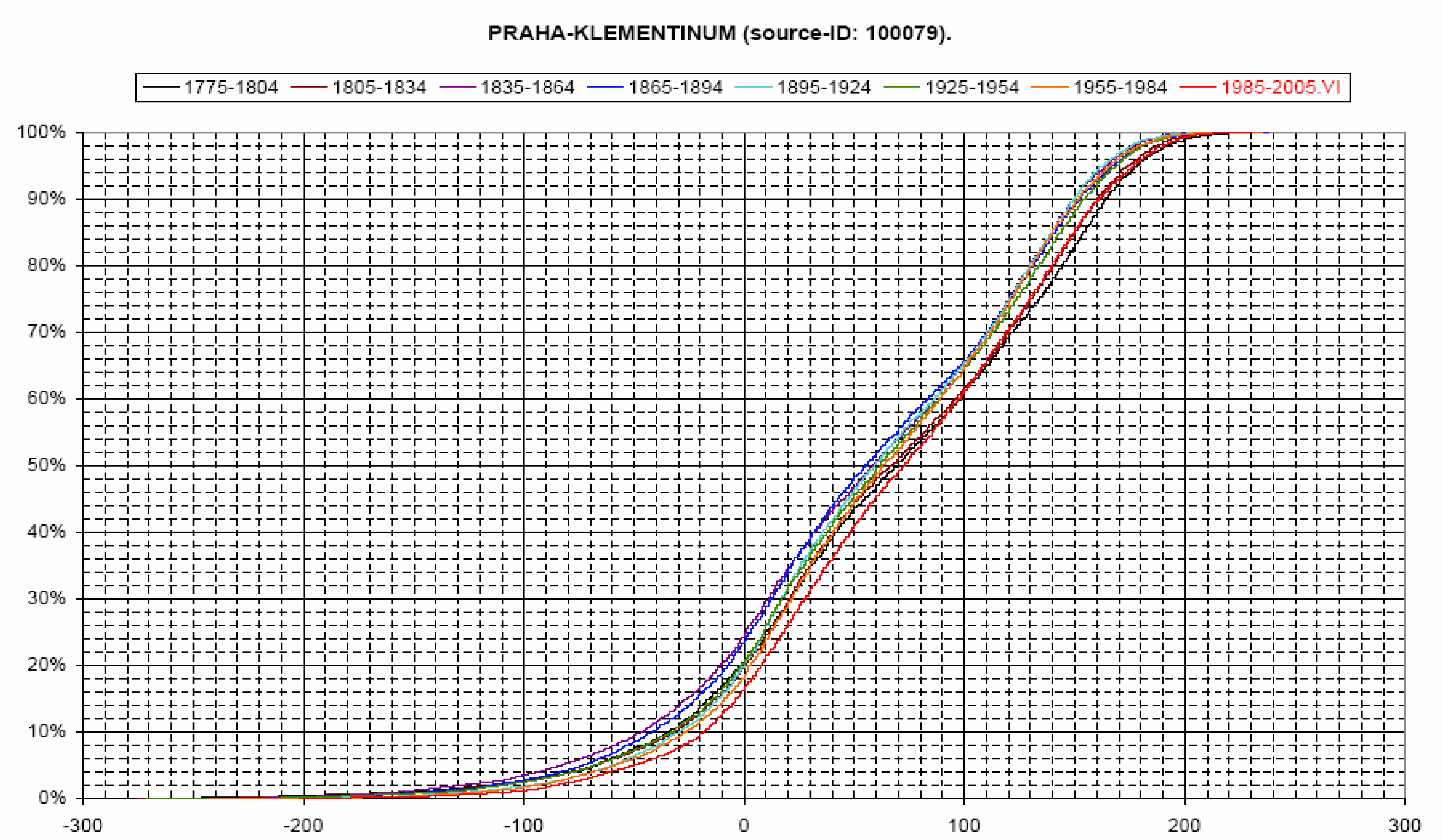
PRAHA-KLEMENTINUM (source-ID: 100079).
1775-1804
1805-1834
1835-1864
1865-1894
1895-1924
1925-1954
1955-1984
1985-2005.VI
100%
90%
80%
70%
60%
50%
40%
30%
20%
10%
0%
-300
-200
-100
0
100
200
300

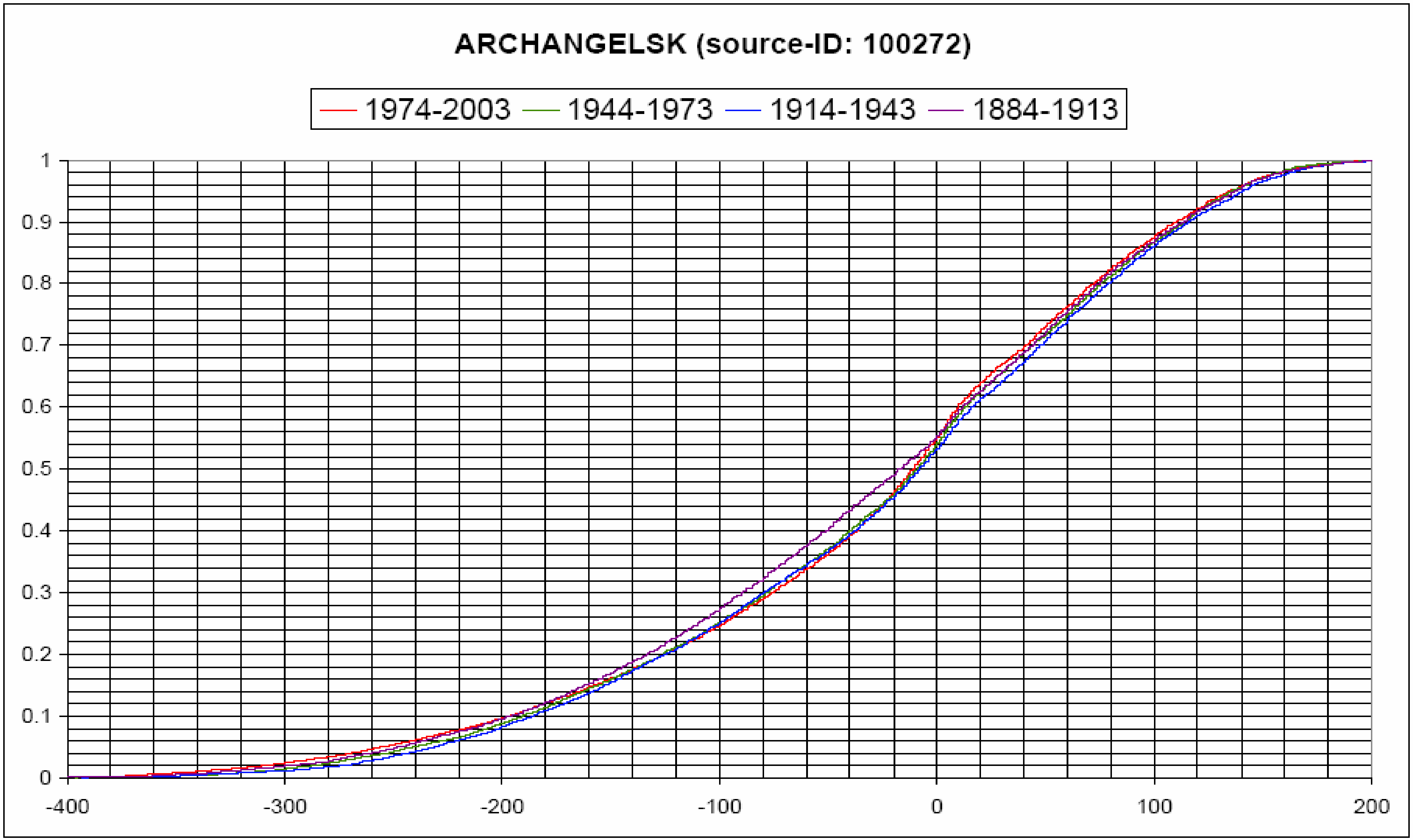
ARCHANGELSK (source-ID: 100272)
1974-2003
1944-1973
1914-1943
1884-1913
1
0.9
0.8
0.7
0.6
0.5
0.4
0.3
0.2
0.1
0
-400
-300
-200
-100
0
100
200

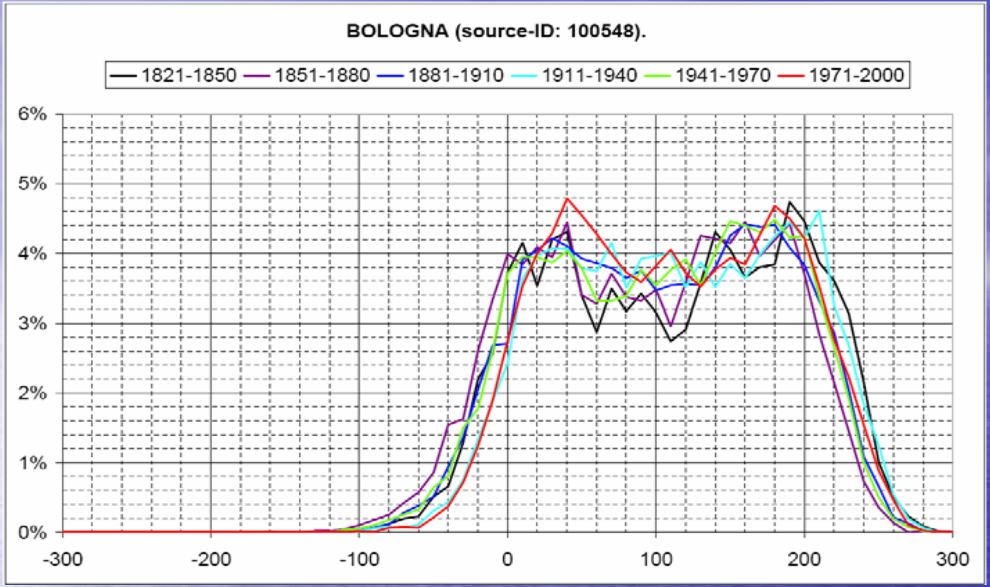
BOLOGNA (source-ID: 100548).
1821-1850
1851-1880
1881-1910
1911-1940
1941-1970
1971-2000
6%
5%
4%
3%
2%
1%
0%
-300
-200
-100
0
100
200
300

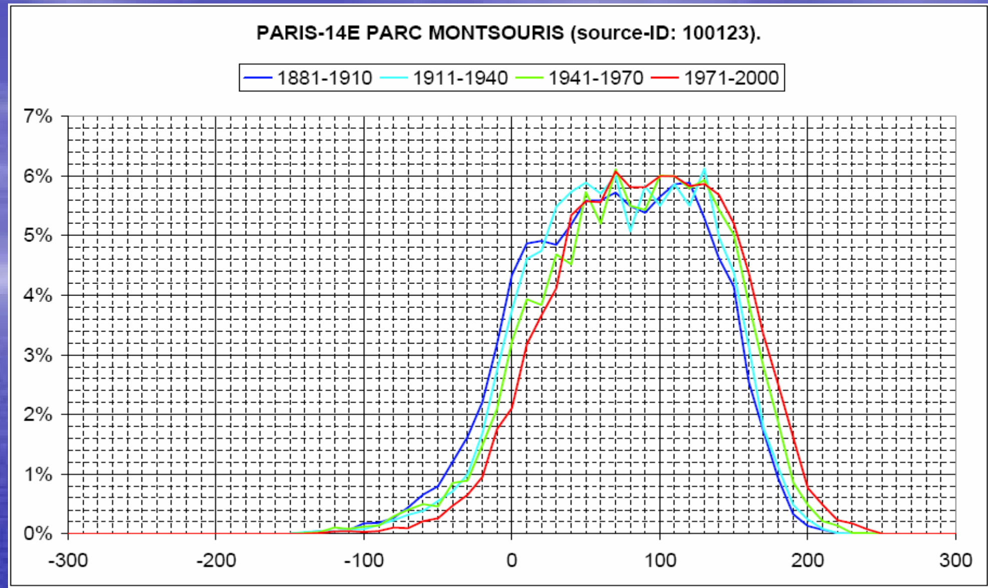
PARIS-14E PARC MONTSOURIS (source-ID: 100123).
1881-1910
1911-1940
1941-1970
1971-2000
7%
6%
5%
4%
3%
2%
1%
0%
-300
-200
-100
0
100
200
300

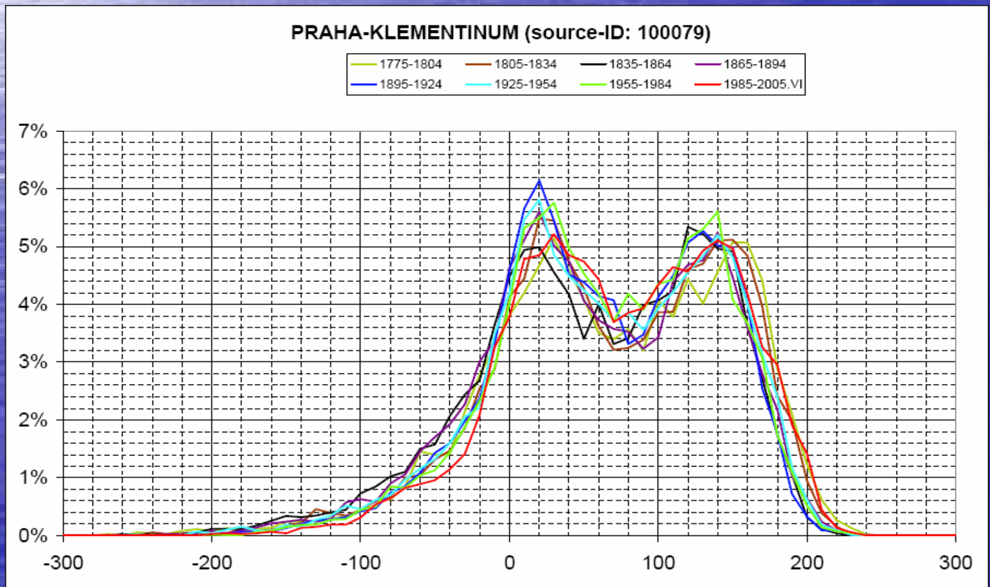
PRAHA-KLEMENTINUM (source-ID: 100079)
1775-1804
1805-1834
1835-1864
1865-1894
1895-1924
1925-1954
1955-1984
1985-2005.VI
7%
6%
5%
4%
3%
2%
1%
0%
-300
-200
-100
0
100
200
300

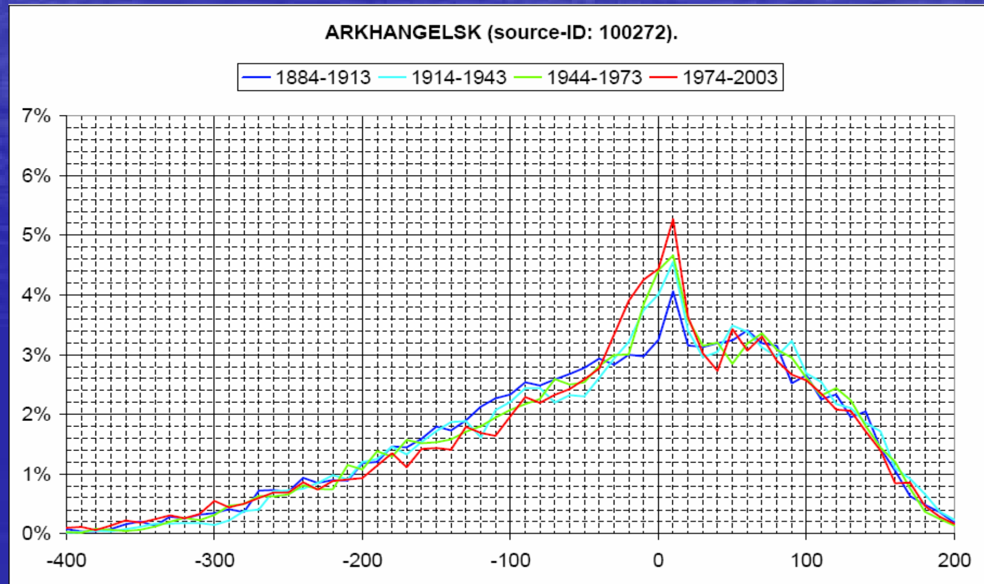
ARKHANGELSK (source-ID: 100272).
1884-1913
1914-1943
1944-1973
1974-2003
7%
6%
5%
4%
3%
2%
1%
0%
-400
-300
-200
-100
0
100
200

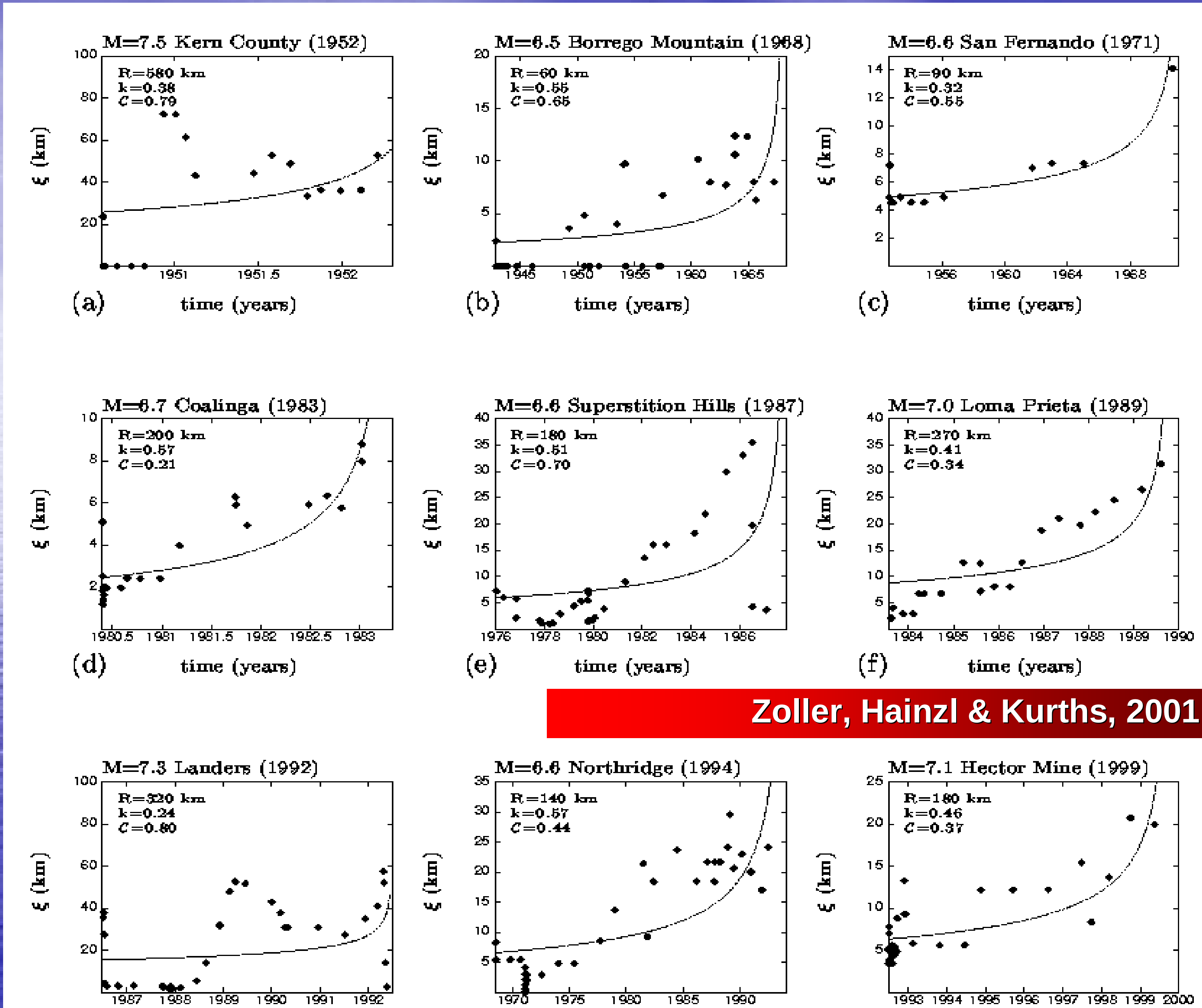

Zoller, Hainzl & Kurths, 2001

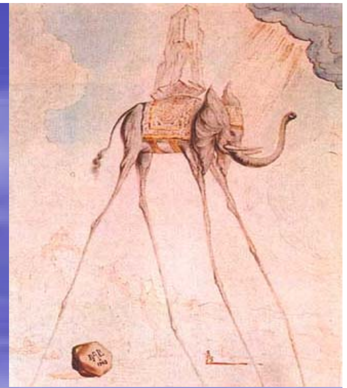

Does "the best fit" model fit the data at all ?